

Aquatic animal propulsion of high hydromechanical efficiency

By M. J. LIGHTHILL

Department of Applied Mathematics and Theoretical Physics,
University of Cambridge

(Received 1 January 1970)

This paper attempts to emulate the great study by Goldstein (1929) ‘On the vortex wake of a screw propeller’, by looking for a dynamical theory of how another type of propulsion system has evolved towards ever higher performance. An ‘undulatory’ mode of animal propulsion in water is rather common among invertebrates, and this paper offers a preliminary quantitative analysis of how a series of modifications of that basic undulatory mode, found in the vertebrates (and especially in the fishes), tends to improve speed and hydromechanical efficiency.

Posterior lateral compression is the most important of these. It is studied first in ‘pure anguilliform’ (eel-like) motion of fishes whose posterior cross-sections are laterally compressed, although maintaining their depth (while the body tapers) by means of long continuous dorsal and ventral fins all the way to a vertical ‘trailing edge’. Lateral motion of such a cross-section produces a large and immediate exchange of momentum with a considerable ‘virtual mass’ of water near it.

In §2, ‘elongated-body theory’ (an extended version of inviscid slender-body theory) is developed in detail for pure anguilliform motion and subjected to several careful checks and critical studies. Provided that longitudinal variation of cross-sectional properties is slow on a scale of the cross-sectional depth s (say, if the wavelength of significant harmonic components of that variation exceeds $5s$), the basic approach is applicable and lateral water momentum per unit length is closely proportional to the square of the local cross-section depth.

The vertical trailing edge can be thought of as acting with a lateral force on the wake through lateral water momentum shed as the fish moves on. The fish’s mean rate of working is the mean product of this lateral force with the lateral component of trailing-edge movement, and is enhanced by the virtual-mass effect, which makes for good correlation between lateral movement and local water momentum. The mean rate of shedding of energy of lateral water motions into the vortex wake represents the wasted element in this mean rate of working, and it is from the difference of these two rates that thrust and efficiency can best be calculated.

Section 3, still from the standpoint of inviscid theory, studies the effect of any development of discrete dorsal and ventral fins, through calculations on vortex sheets shed by fins. A multiplicity of discrete dorsal (or ventral) fins might be

thought to destroy the slow variation of cross-sectional properties on which elongated-body theory depends, but the vortex sheets filling the gaps between them are shown to maintain continuity rather effectively, avoiding thrust reduction and permitting a slight decrease in drag.

Further advantage may accrue from a modification of such a system in which (while essentially anguilliform movement is retained) the anterior dorsal and ventral fins become the only prominent ones. Vortex sheets in the gaps between them and the caudal fin may largely be reabsorbed into the caudal-fin boundary layer, without any significant increase in wasted wake energy. The mean rate of working can be improved, however, because the trailing edges of the dorsal and ventral fins do work that is not cancelled at the caudal fin's leading edge, as phase shifts destroy the correlation of that edge's lateral movement with the vortex-sheet momentum reabsorbed there.

Tentative improvements to elongated-body theory through taking into account lateral forces of viscous origin are made in §4. These add to both the momentum and energy of the water's lateral motions, but may reduce the efficiency of anguilliform motion because the extra momentum at the trailing edge, resulting from forces exerted by anterior sections, is badly correlated with that edge's lateral movements. Adoption of the 'carangiform' mode, in which the amplitude of the basic undulation grows steeply from almost zero over the first half or even two-thirds of a fish's length to a large value at the caudal fin, avoids this difficulty.

Any movement which a fish attempts to make, however, is liable to be accompanied by 'recoil', that is, by extra movements of pure translation and rotation required for overall conservation of momentum and angular momentum. These recoil movements, a potentially serious source of thrust and efficiency loss in carangiform motion, are calculated in §4, which shows how they are minimized with the right distribution of total inertia (the sum of fish mass and the water's virtual mass). It seems to be no coincidence that carangiform motion goes always with a long anterior region of high depth (possessing a substantial moment of total inertia) and a region of greatly reduced depth just before the caudal fin.

The theory suggests (§5) that reduction of caudal-fin area in relation to depth by development of a caudal fin into a herring-like 'pair of highly sweptback wings' should reduce drag without significant loss of thrust. The same effect can be expected (although elongated-body theory ceases to be applicable) from widening of the wing pair (sweepback reduction). That line of development of the carangiform mode in many of the Percomorphi leads towards the lunate tail, a culminating point in the enhancement of speed and propulsive efficiency which has been reached also along some quite different lines of evolution.

A beginning in the analysis of its advantages is made here using a 'two-dimensional' linearized theory. Movements of any horizontal section of caudal fin, with yaw angle fluctuating in phase with its velocity of lateral translation, are studied for different positions of the yawing axis. The wasted energy in the wake has a sharp minimum when that axis is at the 'three-quarter-chord point', but rate of working increases somewhat for axis positions distal to that. Something like an optimum regarding efficiency, thrust and the proportion of thrust de-

rived from suction at the section's rounded leading edge is found when the yawing axis is along the trailing edge.

This leads on the present over-simplified theory to the suggestion that a hydro-mechanically advantageous configuration has the leading edge bowed forward but the trailing edge straight. Finally, there is a brief discussion of possible future work, taking three-dimensional and non-linear effects into account, that might throw light on the commonness of a trailing edge that is itself slightly bowed forward among the fastest marine animals.

1. Introduction

Lighthill (1969) gave a general survey of the hydromechanics of aquatic animal propulsion, composed with the help of zoological colleagues to be as far as possible equally restrained in its presuppositions of hydromechanical and of zoological knowledge in the reader. An important concept in that survey was the hydromechanical efficiency η of an animal's propulsive flexural movements. This has a definition similar to that of the Froude efficiency of a propeller; in fact,

$$\eta = U\bar{P}/\bar{E}, \quad (1)$$

where U is the mean forward velocity, \bar{P} is the mean thrust required to overcome what viscous drag the animal would sustain for forward velocity U if it remained rigid and symmetrical, and \bar{E} is the mean rate at which the flexural movements do work against the surrounding water.

The survey includes a discussion of aquatic propulsion in some twenty classes within the animal kingdom, as well as a more extensive investigation within one class, that of the fishes. The most prominent method of propulsion is the undulatory mode, in which a transverse wave, normally of increasing amplitude, passes backwards along the body from head to tail. This propulsive method, together with various modifications of it, has been successful for motion at both high and low values of the Reynolds number, R , based on the animal's length and forward velocity. Alternative methods, such as ciliary propulsion at low R , and propulsion by jet reaction at high R , have been found more limited in scope and application.

From another point of view, the survey suggests a division of modes of aquatic propulsion into two categories: high-efficiency and low-efficiency, with the separation between them occurring at around $\eta = 0.5$. Essentially, this is a division within the undulatory mode (together with its modifications), because propulsive modes limited to low R like ciliary propulsion seem to be necessarily of low η on such a criterion, while propulsion by the reaction of a jet of velocity U_j has a low Froude efficiency if U_j is a substantial multiple of U , as seems generally to be found in aquatic animals.

Even within the field of undulatory propulsion at relatively high R , a distinction between 'good hydromechanical shapes' with high η and 'bad' ones with low η was already made in the survey. Typical 'bad hydromechanical shapes' for undulatory propulsion at high R include those with roughly circular cross-sections (like most terrestrial snakes) while probably for low to moderate R (say $< 10^3$) all shapes are in this sense 'bad'.

Some excellent theoretical studies of the undulatory mode of propulsion in bad hydromechanical shapes have been made, notably by Taylor (1952) and by Gray & Hancock (1955). Lighthill (1969, §13) summarizes these in an approximate, simplified form. Their essential assumption is that the instantaneous force between the water and a section of the animal's body is the same as when that section moves steadily through the water at the same relative vector velocity. This assumption is particularly good at low R , when viscous forces dominate over inertia.

It is often assumed that this 'quasi-static' theory of undulatory propulsion is equally good at high R . This, however, is not necessarily the case, since it neglects those additional forces required in unsteady motion to accelerate water close to the body section, the mass of water which effectively must be accelerated being that usually described as the 'virtual mass'. Actually, the 'good hydromechanical shapes' seem to be precisely those which are able to improve greatly their propulsive efficiency η by utilizing this virtual-mass effect.

For 'elongated' animals (those whose length very greatly exceeds their other dimensions) Lighthill (1969), using theoretical ideas developed by Lighthill (1960), showed that it is the animals (almost exclusively vertebrates) that have developed transverse compression at the posterior end which can use the virtual-mass effect to improve propulsive efficiency. 'Compression' here means the flattening of the cross-section into a posterior edge or 'trailing edge', and 'transverse compression' signifies compression occurring in that transverse direction in which are made the undulatory displacements that are propagated backwards as the propulsive wave. It is of course lateral (side-to-side) undulations that typical aquatic vertebrates, including most fishes, amphibia and reptiles, use for propulsion, and the characteristic lateral compression at the posterior end of many of these improves hydromechanical efficiency, but, where undulations are dorso-ventral (that is, vertical) as in cetacean mammals, dorso-ventral posterior compression is required.

Posterior transverse compression is important because it permits the virtual mass for the transverse motions of the body section in the water to have a substantial value even at the posterior end, without that very large hydromechanical resistance that would be associated with any blunt backward-facing base. The propulsive benefits of such a substantial trailing-edge virtual mass are given a rather simple mechanical interpretation in §4 of Lighthill (1969), but the point is so important that it must be further developed in the present paper. In particular, those other conditions besides transverse compression which must be satisfied, essentially by the form of the undulatory mode itself in various types of animal, require further study.

Characteristic propulsive modes in the great majority of fishes (for some of the principal exceptions see Lighthill (1969, §§10 and 11)) are broadly divided into two classes: anguilliform and carangiform. Fishes using the anguilliform mode have the whole body flexible, and the propulsive wave travelling from head to tail has an amplitude which, although increasing posteriorly, is significant all along the fish's length. Carangiform propulsion, by contrast, means propulsion in which the amplitude of undulation becomes significant only in the posterior

half, or even one-third, of the length of the fish; the remainder of the fish's body is relatively inflexible.

The mechanics of anguilliform propulsion is, perhaps, simplest in those eels (including *Anguilla* from which the mode's name is derived) and other animals that possess long continuous dorsal and ventral fins whose cross-sectional depth (taking body and both fins into account) either increases or remains substantially constant all the way to the (vertical) trailing edge. It is with this group of animals that theoretical study of anguilliform propulsion begins in §2 below. As elsewhere in this paper, the exposition is confined to cases of only moderate amplitude of undulation, permitting the simplification of Lighthill (1960, 1969) which considers the only significant relative motions of different parts of the fish to be in the lateral direction. Not only the mean forces produced by the undulations but also fluctuations about those means are estimated, and related to the lateral water motions produced adjacent to the body and in the vortex wake.

Anguilliform propulsion is additionally found, however, in several groups of fishes, such as catfishes (see Lighthill (1969) for a fuller enumeration), which possess discrete dorsal and ventral fins behind which the total cross-sectional depth falls to considerably reduced values before increasing again at the tail to a caudal-fin trailing edge of, approximately, the same depth again. In these fishes there are vortex sheets shed already behind the dorsal and ventral fins, and the forces referred to above are modified in an interesting way (investigated in §3) by the free development of those vortex sheets. Mean propulsive force and its efficiency can, it is shown, both be increased under such circumstances, even though the vorticity becomes 'bound' once more on to the caudal fin before it is discarded into the wake.

The same elongated-body theory that is suitable for studying anguilliform motion is useful also for studying the fundamental modification of that motion (with the undulations confined to a tail region) that we call carangiform. This propulsive mode is, in the main, investigated in §4, which demonstrates why the modification is advantageous from the point of view of propulsive efficiency.†

This advantage, however, is not reaped unless there is a very large reduction of depth (that is, a 'necking' in lateral view) in the region, just anterior to the caudal fin, where the undulation amplitude has a steeply increasing gradient. Farther forward still the total depth of dorsal fin, body and ventral fin can, and indeed should, be as large as that of the trailing edge, with comparable depths maintained for a considerable length of fish body. Complications such as those mentioned above, with a vortex sheet shed from the dorsal and ventral fins, are absent however because those fins do not significantly take part in carangiform undulation.

The calculations in §§2-4 are limited to a fish pursuing a straight path to which no part of it is inclined at more than a moderate angle (say, less than 30°), so that to good approximation the important relative motions of different parts of the fish are in the lateral direction. One advantage of setting out calculations on this basis in careful detail is that they can be conducted either in the form

† The exception is a particular variant of the carangiform mode, to which elongated-body theory is inapplicable, and which is treated in §5.

of a rigorous, but complicated, perturbation expansion in which the forces acting between the body and the water are obtained by integrating surface pressure distributions, as in the appendix to Lighthill (1960), or as here by some rather more tentative, but simpler, considerations of bulk momentum and energy, and the two methods give identical results, which adds to one's confidence in both.

A less restrictive analysis is desirable, however, partly because amplitudes used by fishes swimming at their top speed are in reality considerably greater, with tails inclined by as much as 60° to the direction of motion. Furthermore, it is of great interest to be able to analyse turning manoeuvres. With these objects in mind, a new version of elongated-body theory is being prepared for future publication, based on similar considerations of bulk momentum and energy to those whose reliability is verified here, but using far less restrictive geometrical assumptions.

The crude idea expounded so far, that for the 'bad hydromechanical shapes' quasi-static values of resistance to the motion of body sections may properly be used, as in Taylor (1952) and Gray & Hancock (1955), while for 'good hydro-mechanical shapes' the virtual-mass effects of elongated-body theory dominate and resistance forces are negligible by comparison, is obviously exaggerated. It would be most desirable to work out a theory combining the two effects. Only a beginning is here made on this problem; see especially §4, where an idea of Lighthill (1960) for effecting such a combination is pursued somewhat further.

The last section of this paper is devoted to investigations arising from the principal conclusion which Lighthill (1969) draws (see especially his figure 6): namely that all the fastest marine animals, and in particular a certain group of bony fishes that includes the tunnyfishes, a certain group of unusually fast sharks, and also most of the cetacean mammals, have adopted an essentially carangiform mode of propulsion but with tails greatly modified along essentially identical lines. These are high-aspect-ratio tails of crescent-moon shape, and such a tail is often called 'lunate' whether it is a vertical fish caudal fin or a horizontal cetacean tail-fluke. Lighthill gives reasons for supposing that these fast animals from very different lines of evolution have 'converged' upon the lunate tail (see also Kramer 1960, figure 18) primarily because it possesses hydromechanical advantage, and indicates ways in which its hydromechanics may be analysed.

It is impossible to use elongated-body theory to study lunate-tail hydro-mechanics, because elongated-body theory assumes that the water is set into motion by body actions that, essentially, are distributed along the direction of motion, so that each vertical slice of water perpendicular to that direction is influenced primarily by body actions close to the slice. By contrast, the action of the propulsive lunate tail is spread out at right angles to the direction of motion; vertically in the case of the fishes. The large vertical extent of the fish's tail makes the assumptions of elongated-body theory untenable, because changes in the body action on neighbouring water slices perpendicular to the direction of motion are altogether too abrupt for their influences to be regarded as acting independently.

On the other hand, the action of the lunate vertical fin's lateral motion on different *horizontal* slices of water is far more gradually varying, and can more

reasonably be regarded as mutually independent to a first approximation. This suggests treating the lunate tail by the two-dimensional theory of oscillating aerofoils. Lighthill (1969, §§8 and 9) proposes as a first approximation this method, taking into account only the cross-stream (in the case of fishes, vertical) components of wake vorticity, although he suggests as a more accurate (but more difficult) method of calculation a 'lifting-line' theory that would also take the streamwise components into account. The latter theory would give a lower, more accurate, estimate of efficiency through not ignoring parts of the wake energy associated with the streamwise vorticity.

It seems clear that, if indeed two-dimensional oscillating-aerofoil theory is of any value as a first approximation in fish hydrodynamics, then it is in this application to lunate-tail propulsion. By contrast, any attempt to study propulsion in the more normal elongated fishes by investigating an 'analogous two-dimensional fish' cannot give answers that are even approximately reliable because the basic assumption of two-dimensional theory, that body actions are spread out at right angles to the direction of motion, is the complete opposite of the truth for an elongated fish. Accordingly, the values of an aerofoil frequency parameter $\omega c/U$ (based on radian frequency ω and forward speed U) that are relevant to fish propulsion must involve a chord c equal not to the fish length l but to the lunate tail's dimension in the direction of motion. Such values of $\omega c/U$ are typically less than 1, even though $\omega l/U$ is normally around 10.

A general characteristic of the carangiform mode (Lighthill 1969, §5) is that the oscillations of the caudal fin's angle of attack and lateral velocity are in phase with one another. Accordingly, Lighthill made lunate-tail calculations, of which he gave the results in his figure 9, based on assuming that the postulated two-dimensional aerofoil sideslips with oscillating velocity $W \cos \omega t$ and yaws with the in-phase oscillating angle of attack $(\theta W/U) \cos \omega t$. In these calculations the axis of the yawing oscillation was taken for simplicity as the central (or 'half-chord') axis of the aerofoil; the parameter θ was described as a 'proportional feathering'. There is no thrust when $\theta = 1$, but although thrust increases as θ falls away from 1 the fin generates what thrust there is with greatest efficiency if θ is not too far below 1. When θ falls to zero, efficiency is reduced (even on this two-dimensional theory, neglecting streamwise vorticity, it is down to 0.65 for $\omega c/U = 1$) but thrust itself is then at a maximum.

This case $\theta = 0$ is one of pure sideslip without yawing, so that none of the thrust can come from any difference of pressure between the two sides of the fin. Under these circumstances (when actually thrust is greatest though it is not generated with great efficiency), the whole thrust comes from leading-edge suction; that is, from the action on the rounded leading edge of the reduced pressure in the water swirling round it. When θ is non-zero, not all but a large part of the thrust comes from leading-edge suction, and to realize it a bluntly rounded leading edge, such as is indeed found in all the animals with lunate tails, is necessary.

In §5 below, the calculation just described is repeated with a more general position of the yawing axis. The dependence of efficiency on this position is predicted as unexpectedly sensitive. For given amplitudes the wasted wake energy

has a minimum when the axis is at the three-quarter-chord point (that is, three times as far from the leading edge as from the trailing edge). Rate of working increases somewhat for axis positions distal to that point, and an optimum for both thrust and efficiency places the axis very close to the trailing edge.

This new result seems to have definite relevance to the question of why the lunate tail should be hydromechanically efficient. If a caudal fin were yawing as a whole about a single axis, and if two-dimensional theory could be applied to each section, we could infer that good thrust with good efficiency would best be obtained if the trailing edge ran straight along the axis of yaw. For a tapered fin shape this would mean that the trailing edge was straight although the leading edge was considerably bowed forward. This degree of departure from 'straight wing' conditions (when the leading edge would be bowed forward but the trailing edge would be bowed backward to an equal extent) is in the right direction, although it does not go far enough; possibly a fully three-dimensional theory might explain the fact that the trailing edge is even slightly bowed forward.

The most promising type of three-dimensional theory may be a sort of lifting-line theory in which the local flow around each cross-section is taken as a two-dimensional flow but with a local angle of attack influenced by the whole pattern of wake vorticity. The form of the two-dimensional theory as explained in §6 has been selected to facilitate its possible use in three-dimensional calculations of this kind.

In the meantime, the general conclusion concerning the trailing edge may, perhaps, find application to other aspects of animal locomotion. For example, if the flapping of a bird's wings were approximated on a two-dimensional theory as a combination of a pitching oscillation (superimposed, as in figure 7 of Lighthill (1969), on the uniform angle of attack required for weight support) and a heaving motion whose velocity oscillates in phase with the pitch angle, then the predicted propulsive efficiency would be greatest if the pitch axis were along the trailing edge.

It will be seen that §§2 to 5 of this paper form a sort of mathematical appendix to the generally non-mathematical discussion of Lighthill (1969) and of this introduction.

2. The pure anguilliform mode of propulsion

Fishes may be said to adopt a 'pure' anguilliform mode of propulsion when, like *Anguilla vulgaris*, they possess long continuous dorsal and ventral fins whose cross-sectional depth (taking body and both fins into account) is maintained, or even increases, all the way to the posterior end; there, such taper as may appear in lateral view is so abrupt that to a close approximation the fish body may be regarded as terminating in a vertical trailing edge. Such a fish, at its lower speeds of movement, often propels itself by undulations that pass only along the fins, but at its higher speeds makes a close approximation to the pure anguilliform mode, in which a single lateral undulation, involving the body as well as the fins, passes backwards from the head to the tail. This mode is analysed by

'elongated-body theory' (an adaptation of what is called 'slender-body' theory in aeronautics) in the present section.

We first set it out, as Lighthill (1960) did, in a frame of reference moving with the mean speed U of the fish, so that in this frame of reference the fish is making undulatory movements in order to remain in the same average position in a stream whose undisturbed velocity is U , directed along the x -axis. We describe the fish's undulations by reference to a 'stretched straight position' in which the body is perfectly symmetrical about the vertical plane $z = 0$. To hold the fish in the stream in the stretched straight position would require a force equal to the viscous drag D (whose magnitude we can infer from observations of deceleration when a fish of known mass glides rigidly). We investigate how, without any external force, the fish may perform undulations about the stretched straight position which maintain its mean position in the stream, so that they may be said to generate a net thrust P that exactly balances the drag D .

In the stretched straight position, the cross-section of the fish at a distance x from the front end is called S_x by Lighthill (1960), who further supposes that, during undulations, the cross-section is displaced by an amount $h(x, t)$ in the z -direction (in other words laterally). Lighthill (1969) used the notation W for the lateral velocity $\partial h/\partial t$ of a cross-section. We follow him in this, as also in the use of

$$w = \partial h/\partial t + U \partial h/\partial x, \tag{2}$$

rather than the V of Lighthill (1960), to signify the velocity of lateral pushing of a vertical water slice (perpendicular to the x -axis) by the successive cross-sections past which it sweeps with velocity U .

Lighthill (1969, §4) explained in as simple terms as possible why w is considerably smaller than W at the trailing edge if in its neighbourhood the undulation has developed into a travelling wave of velocity V only moderately greater than U and of constant amplitude. In the language of partial derivatives this is because $\partial h/\partial t + V \partial h/\partial x$ is then zero, and so equation (2) gives

$$w = W(V - U)/V. \tag{3}$$

It was noted that w/W should be relatively small for good efficiency, but must not be too small if thrust is to be adequate to overcome the viscous drag D .

Associated with the lateral pushing of a water slice at velocity w is a certain lateral momentum in the water slice. When such pushing begins, this momentum rises *immediately* to a value mw per unit length (more strictly, that momentum is communicated to the water by a signal propagated at the speed of sound, which may however be taken infinite in the present context), where m is the virtual mass per unit length of fish. Continued pushing will produce a certain amount of increase above this value, through the action of viscous forces, especially in the production of streamwise vorticity shed in the cross-stream flow, and this is investigated in §4, but here the momentum present without any such augmentation is first studied.

Elongated-body theory as developed by Lighthill (1960), assuming that rates of change of cross-sectional dimensions along the fish's length are small, and that undulatory movements do not much distort the streamwise distribution of fish

mass and are not too abruptly varying, arrives at the conclusion that for a particular cross-section S_x we may estimate m as the virtual mass per unit length (there written ρA) for an infinite rigid cylinder C_x with the same cross-section. This quantity is easily obtained from the complex-variable theory of two-dimensional irrotational flow for a variety of cross-sectional shapes relevant to different groups of fish.

An interesting conclusion from such calculations is that m depends to a rough approximation only on the depth s of the cross-section. Indeed, if we write

$$m = \frac{1}{4}\pi s^2 \rho \beta, \quad (4)$$

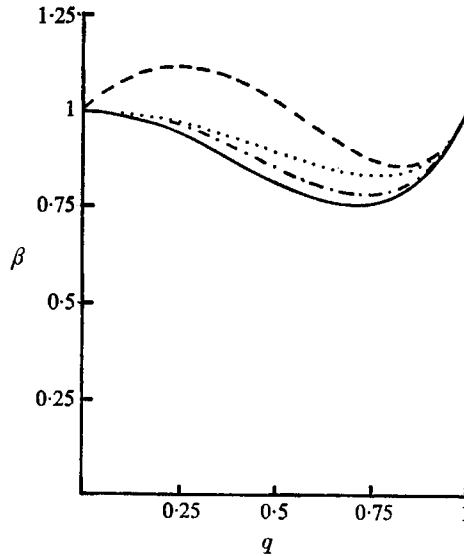


FIGURE 1. Virtual-mass coefficients β , defined in equation (4), for cross-sections such that a fraction q of the total depth s is occupied by fish body and the remainder by dorsal and/or ventral fins., elliptical body cross-section (axis-ratio 2) with equal dorsal and ventral fins. Curves for circular body cross-section: —, equal fins; - · - ·, fin depths in ratio 3:1; ----, one fin only.

where ρ is the water density, then the non-dimensional parameter β varies little from 1. It is exactly 1 for an elliptic cross-section of any eccentricity, ranging from the nearly circular section of the anterior portions of many eels, through the highly eccentric elliptical section of for example a herring, to the quite flat section characteristic of a trailing edge. Figure 1 shows the extent to which β departs from 1 for some other typical cross-sections.

These include cross-sections in which a fraction q of the total depth s is occupied by a body whose section is a circle, or an ellipse with major axis vertical, and the remainder by two vertical fins (dorsal and ventral) of negligible thickness. When the fins are of equal depth (that is, $\frac{1}{2}(1-q)s$ each) the plain line shows that β is 1 for $q = 0$ or 1 but falls to a minimum of 0.75 for $q = 0.7$ in the case of a circular body, while departing much less from 1 when the body is elliptical (dotted line). Results (chain-dotted line) for fins of unequal depths $\frac{3}{4}(1-q)s$ and $\frac{1}{4}(1-q)s$, and also (broken line) for a single fin of depth $(1-q)s$, show that even for a

circular body the departure of β from 1 is reduced in these cases, while corresponding curves for an elliptical body (not shown) involve, as would be expected, still smaller departures from 1.

The importance of confidently knowing the virtual mass per unit length m makes it desirable, however, to probe further the inference from elongated-body theory that, at the section S_x , it is the same as for an infinite rigid cylinder C_x with the same cross-section. How far does this need correction due to two facts: (i) that the fish body is flexible so that different cross-sections push the water with different velocities, and (ii) that its cross-section is non-uniform? Fairly simple answers to these questions can be obtained in the special case when cross-sections are circular; these answers indicate that corrections are then not large provided that significant harmonic components of cross-section shape or velocity along the fish have wavelengths λ of at least $5s$.

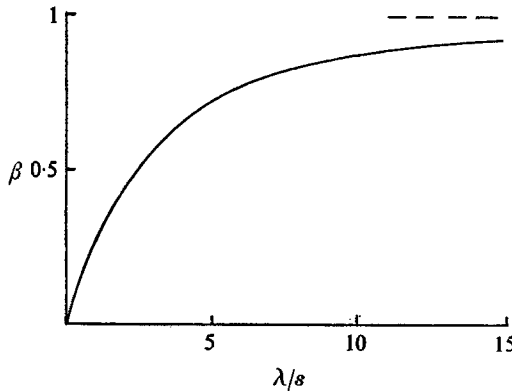


FIGURE 2. Virtual-mass coefficient β as a function of the ratio λ/s of wavelength to depth of fish cross-section (assumed circular).

Such answers are obtained from solutions of Laplace's equation in cylindrical polar co-ordinates (x, r, θ) proportional to $K_1(kr) \cos \theta \cos kx$, where $k = 2\pi/\lambda$. If, for example, a cylinder of uniform circular cross-section pushes the water in the direction of the axis $\theta = 0$ (corresponding to the z -axis in Cartesian co-ordinates) with a velocity varying like $\cos kx$, these solutions allow us to calculate the virtual mass per unit length in the form (4) with

$$\beta = K_1(\pi s/\lambda)/[-(\pi s/\lambda) K_1'(\pi s/\lambda)]. \tag{5}$$

Figure 2 shows that this β is within 25 % of 1 for $\lambda > 5s$. Similar calculations on the effect of a particular harmonic component of variation of the cross-section depth, under conditions of uniform pushing, show that the greatest departure of β from 1 is then the same as equation (5) would give but further reduced by the ratio of the amplitude to $\frac{1}{2}s$, a ratio which inherently must be less than 1.

These indications for circular cross-sections S_x , that the virtual mass is to a rough approximation the same as for a rigid cylinder C_x with the same cross-section if wavelengths of significant variations in the streamwise direction exceed $5s$, can probably be relied on also for various more flattened (that is, laterally

compressed) types of cross-section. These, indeed, should be *more* able to 'get a grip on' the water near them in a way such that the lateral water motion simply reflects that of the local body cross-section. Therefore, since in pure anguilliform motions a typical wavelength of undulation (see, for example, figure 4 of Lighthill 1969) is considerably more than $5s$, it is reasonable to treat them all by elongated-body theory, founded on the above approximations to virtual mass.

The z -component of the force with which the fish acts on a water slice, per unit distance in the x -direction, must equal the rate of change of z -component of momentum of the water slice as it sweeps past the undulating fish at velocity U . This is

$$Z = \left(\frac{\partial}{\partial t} + U \frac{\partial}{\partial x} \right) [m(x)w(x, t)], \quad (6)$$

where $m(x)$ is given by equation (4) essentially in terms of the depth $s(x)$ of the cross-section S_x (since β is close to 1) and $w(x, t)$ by equation (2). In (6), departures of the x -component of water-slice velocity from U can reasonably be neglected since they are of the second order in the undulations (being of the order of products of transverse velocities w with local angles of body twist out of the stretched straight position).

The rate, E , at which the fish is doing work through its transverse movements with velocity $\partial h/\partial t$, exerting forces Z per unit length, is

$$E = \int_0^l Z \frac{\partial h}{\partial t} dx, \quad (7)$$

and by equation (6) for Z and equation (2) for w this can be written

$$\begin{aligned} E &= \int_0^l \left(\frac{\partial}{\partial t} + U \frac{\partial}{\partial x} \right) \left(mw \frac{\partial h}{\partial t} \right) dx - \int_0^l mw \frac{\partial w}{\partial t} dx \\ &= \frac{\partial}{\partial t} \int_0^l \left(mw \frac{\partial h}{\partial t} - \frac{1}{2}mw^2 \right) dx + U \left[mw \frac{\partial h}{\partial t} \right]_{x=l}. \end{aligned} \quad (8)$$

The integrated term in (8) (last term on the right-hand side) involves a contribution only from the posterior end $x = l$, where the lateral compression makes m non-zero; by contrast, m becomes zero at the anterior end $x = 0$.

This last term in (8) is particularly important because only through it can the fish exert any mean power. The first term, by contrast, is merely the time derivative of a fluctuating quantity so that its time mean is zero.

Lighthill (1969) gives a simple mechanical interpretation of this important last term, which is $UmwW$ in the notation he uses. Here, mw is the lateral momentum per unit length in the water near the trailing edge, and so Umw is the rate of shedding of that momentum into the vortex wake per unit time, which, effectively, is a lateral force with which the trailing edge acts on the wake, doing work at a rate $UmwW$ because its lateral velocity is W . Equation (3) shows this rate of working to be always positive and to have a mean value simply proportional to the mean square of the trailing-edge lateral velocity W .

We need to ask, however, why this simple mechanical argument yields correctly only the mean value of the rate of working, and not the instantaneous value given by (8), including the first term on the right-hand side. The reason is

that the undulating fish does not do work only on the wake. Part of its rate of working involves exchange of energy with water that has not yet reached the wake. The total energy of such water ahead of the trailing edge fluctuates up and down, so that its rate of change is not instantaneously zero, although it has a zero mean rate of change over a long time (or over a single period of oscillation).

This interpretation of equation (8) can be verified if it is recast, using (2), as

$$E - U[mwW]_{x=l} = \frac{\partial}{\partial t} \int_0^l \left(\frac{1}{2}mw^2 - Umw \frac{\partial h}{\partial x} \right) dx. \quad (9)$$

This equates the rate of working by the fish, minus the rate at which it does work on the wake, to the rate of change of an energy integral. In this integral the first term represents the energy of water motions in the y - and z -directions. In the frame of reference used, however, there are also comparable fluctuations in the energy of water motions in the x -direction.

Specifically, when unit mass of water makes a small change in its velocity from U to $U+u$, there is an energy change which to a first approximation is Uu . Therefore, when a large body of water moving with velocity U suffers a non-uniform small perturbation of velocity, the energy change is U times the change in the x -component of momentum. Where the water momentum per unit length due to the fish's transverse motion is mw , but not exactly in the z -direction because the fish body is sloped at an angle $\partial h/\partial x$ to the stretched straight position, there will to first approximation be an x -component of momentum $-mw \partial h/\partial x$ (again per unit length), with a corresponding energy change $-Umw \partial h/\partial x$ which explains the second term inside the integral in (9).

Here we have used an important extension of the basic idea that water momentum, due to relative motion in the z -direction with velocity w of a section S_x of fish, is that of a cylinder C_x with the same cross-section. The extended idea is that if S_x is sloped at a non-zero angle to its stretched straight position then the corresponding cylinder C_x must be thought of as so sloped, with the consequence that the associated momentum, necessarily at right angles to the generators of the cylinder, is sloped back from the z -direction. This extension is fully supported by the arguments in favour of the virtual-mass concept given earlier.

The rate of working E can also be expressed in terms of the thrust P (whose value can therefore be obtained by comparing the two expressions), if we use a different frame of reference; one in which the water far from the fish is at rest. We can then write

$$E = UP + U[\frac{1}{2}mw^2]_{x=l} + \frac{\partial}{\partial t} \int_0^l (\frac{1}{2}mw^2) dx, \quad (10)$$

where the first term on the right is the work done by the fish in simply moving at velocity U in the direction of the thrust P . The second term represents the rate at which kinetic energy of water movements, namely $\frac{1}{2}mw^2$ per unit length of fish, is shed to the wake at the trailing edge. This 'wasted' energy was emphasized by Lighthill (1969, §4). The third term in (10) represents the rate of change of a fluctuating quantity, namely the total kinetic energy (in the new frame of reference) ahead of the trailing edge.

From (9) and (10), by subtraction, we obtain the thrust

$$P = [mw(W - \frac{1}{2}w)]_{x=l} - \frac{\partial}{\partial t} \int_0^l \left(mw \frac{\partial h}{\partial x} \right) dx. \quad (11)$$

Equations (9) and (10) can also be used directly to estimate the hydromechanical efficiency η , given by (1) as $U\bar{P}/\bar{E}$. Using the fact that the mean value of the time derivative of each integral is zero, we obtain

$$\eta = 1 - (\bar{E} - U\bar{P})/\bar{E} = 1 - \frac{1}{2}[\overline{w^2}]_{x=l}/[\overline{wW}]_{x=l}. \quad (12)$$

Provided that w and W at $x = l$ are related by equation (3), this implies that $\eta = 1 - \frac{1}{2}(V - U)/V$. This reinforces the argument of Lighthill (1969) that good efficiency requires w to be considerably smaller than W (and hence V not too much greater than U), although for substantial thrust, as (11) shows, w must certainly not be too small.

Equation (11), however, gives not only the mean, but also the instantaneous value of the thrust P . This value is obtained more easily by the above subtraction method than by any direct physical argument. The latter is possible, however, and is based on the following modified form of (11):

$$P + [Umw \partial h/\partial x - \frac{1}{2}mw^2]_{x=l} = \frac{\partial}{\partial t} \int_0^l (-mw \partial h/\partial x) dx, \quad (13)$$

a form which, we may note, agrees with that derived in a completely independent way (through integrating the distribution of surface pressures obtained by a careful perturbation expansion) in the appendix (see equations (A 21), (A 26) and (A 27)) to Lighthill (1960).

To interpret (13) physically, we note that the right-hand side is the rate of change of the x -component of water momentum in the region anterior to a plane Π through the trailing edge perpendicular to the x -direction. This momentum component changes partly due to the action of the force P between the fish surface and the water, and partly due to momentum transport across Π , represented by the expression in square brackets. In this expression, loss by convection at velocity U of momentum $-mw \partial h/\partial x$ per unit length appears first. The second term represents a loss due to the resultant pressure force acting over the plane Π .

A direct physical argument to derive P is made more difficult by the fact that momentum transfer occurs additionally through the agency of this non-vanishing pressure force. That its value is $\frac{1}{2}mw^2$ follows most easily from the unsteady form of Bernoulli's equation in a frame of reference in which the fluid velocity at large distances is $-w$ in the z -direction; in this frame of reference the fish motion relative to the water is zero at the trailing edge. Then the quadratic terms in Bernoulli's equation give pressures

$$\frac{1}{2}\rho[w^2 - (\partial\phi/\partial y)^2 - (\partial\phi/\partial z)^2] = \rho w(\partial\phi/\partial z + w) - \frac{1}{2}\rho[(\partial\phi/\partial y)^2 + (\partial\phi/\partial z + w)^2], \quad (14)$$

whose resultant can be expressed in terms of the total momentum mw and kinetic energy $\frac{1}{2}mw^2$ per unit length in the field $(\partial\phi/\partial y, \partial\phi/\partial z + w)$ as

$$w(mw) - \frac{1}{2}mw^2 = \frac{1}{2}mw^2. \quad (15)$$

(On the other hand the $-\rho \partial \phi / \partial t$ term in the pressure gives no resultant because for a section symmetrical about $z = 0$ the potential ϕ is an odd function of z .)

The presence of such a resultant pressure force $\frac{1}{2}mw^2$ across the plane Π is inferred again by vorticity considerations in §3, through consideration of how the x -component of momentum in the wake is changing otherwise than by the shedding of momentum from the trailing edge. Other refinements of the theory of this section, specially designed to throw light on evolutionary deviations from pure anguilliform motion, are given in both the subsequent sections.

3. Vortex sheets shed by fins

In this section, we precede a discussion of vortex shedding by fins in general with a discussion of the form of the water flow just behind the trailing edge in pure anguilliform motion. This is the flow carrying those quantities of momentum and kinetic energy predicted in §2 as shed into the wake. It will be evident to certain readers, especially those with aeronautical experience, that this must take the form of a vortex sheet, and specifically (since we are dealing with the low-aspect-ratio limit) one with a distribution of vorticity corresponding to an ‘elliptic distribution’ of velocity potential (minimizing, per unit length of wake, the kinetic energy for given lateral momentum and span).

To see how this follows from the theory of §2, we note that when the cross-section S_x is located at a vertical trailing edge the corresponding cylinder C_x is an infinitely long, infinitesimally thin strip of depth s . The velocity potential ϕ for motion of such a strip with velocity w in the z -direction takes values

$$\phi = \mp w \left[\frac{1}{4}s^2 - (y - y_0)^2 \right]^{\frac{1}{2}} \tag{16}$$

on the sides of strip $|y - y_0| < \frac{1}{2}s$, $z \geq 0$ respectively. Equation (16) exhibits already the elliptic distribution of trailing-edge velocity potential. It means that the vertical velocity component $\partial \phi / \partial y$ changes by an amount

$$\Delta(\partial \phi / \partial y) = 2w(y - y_0) \left[\frac{1}{4}s^2 - (y - y_0)^2 \right]^{-\frac{1}{2}} = -\Xi, \text{ say,} \tag{17}$$

between the $z < 0$ and $z > 0$ sides of the trailing edge.

Such a discontinuity in velocity is equivalent to a vortex sheet, a thin layer in which the x -component of vorticity ξ takes large values, whose integral across the layer is Ξ ; or, since in reality there are boundary layers on both sides of the solid strip, this must actually be the integral of ξ across the two boundary layers. It follows that a perfectly consistent picture of the flow can be built up in which equation (16) represents the cross-flow around the posterior end of the fish (more strictly, around the boundary layers attached to its surface), whereas behind the trailing edge there is a free vortex sheet with the same strength Ξ , with the same values (16) of the velocity potential on the two sides of it, and inducing the same cross-flow around it.

This is a consistent model because (i) such continuity at the trailing edge between the upstream and downstream cross-flows means that variation in cross-flow is gradual there as well as around the main part of the body, which justifies (as in §2) the local use of the two-dimensional form of cross-flow (that around

C_x); (ii) continuity in the integrated x -component of vorticity, Ξ , at the trailing edge is consistent with the solenoidal character of the vorticity field and with the convection of vortex lines with the fluid.

In a frame of reference in which the undisturbed fluid is at rest, the vorticity shed into the wake remains unchanged in magnitude and continues to exhibit the same bodily motion, with velocity w in the z -direction, that is implied by the surface values (16) of velocity potential. At each point in the wake the local value of w (which is linked through equation (17) with the local value of the vortex-sheet strength Ξ) is equal to the value that w had at the trailing edge when the trailing edge passed that point. This implies a certain non-uniformity in w along the wake, reflecting the variability with time in the trailing-edge value of w .

The vorticity in the sheet is rotated about the y -direction by any variation of w with x , the angular velocity of rotation of vortex lines being $-\partial w/\partial x$. As this happens the direction of the associated momentum, mw per unit length, also rotates; this momentum is in a direction close to the z -direction, but the twisting causes x -momentum to appear in addition, at a rate $-mw\partial w/\partial x$. The total rate of change of wake momentum due to this cause is

$$\int_l^\infty (-mw\partial w/\partial x) dx = [\frac{1}{2}mw^2]_{x=l}, \quad (18)$$

since the fluid is undisturbed at infinity. Equation (18) confirms the value obtained by quite different considerations of pressure distribution in §2 (see especially (15)).

There is no special point in pursuing farther the discussion of the wake in the pure anguilliform motion of animals with continuous dorsal and ventral fins. However, considerations analogous to those just described are relevant also to understanding the wakes from discrete dorsal and ventral fins, with more or less unswept trailing edges, carried by animals performing an essentially anguilliform mode of undulation. In the neighbourhood of a cross-section including such a fin, the velocity potential takes different values on the fin's two sides, just as in (16), corresponding to a vortex sheet of strength $\Xi = -\Delta(\partial\phi/\partial y)$ as in (17). Equations (16) and (17) would only represent their values to good approximation if the body were thin in relation to its depth; corresponding results for rounder bodies can, however, be calculated by complex-variable theory.

Immediately behind the posterior edge of the fin, a vortex sheet of the same strength Ξ must be found, for exactly the reasons described above. In a frame of reference in which the undisturbed water is at rest, this vortex-sheet strength remains unchanging, and has at any point a value proportional to the value of w at the fin's posterior edge when the latter passed the point. In the frame of reference of §2, with the undisturbed water moving at velocity U , the vortex-sheet strength is accordingly a fixed function of $t - (x/U)$ and y .

We apply these considerations first to cod, and those other members of the family Gadidae in the order Anacanthini, which both dorsally and ventrally possess a succession of closely spaced fins, and swim with an essentially anguilliform motion. Behind the anterior dorsal fin such a vortex sheet will be found, filling the gap between it and the second dorsal fin, and producing a far greater continuity in the cross-flow than would be expected from the geometry.

At the second dorsal fin, this vortex sheet gets mixed with the boundary layer. Such incident streamwise vorticity should not significantly influence the cross-flow, or the overall vortex-sheet strength over that fin, since those are uniquely determined by the local value of w . Accordingly the presence of the detached vortex sheet between the two fins is purely a local modification, which influences little the flow behind it. Other gaps between fins are similarly filled in by vortex sheets.

When, as in many of the Gadidae, these gaps are small (for the case of large gaps, see below), the dynamical effect of the vortex sheet is practically the same as if the dorsal fin were continuous. Actually any difference between the cross-flow around a body section S_x including part of the vortex sheet and that which would be present if the vortex sheet were replaced by solid fin can only be due to: (i) differences between the body section shape where the vortex sheet was shed and at S_x ; or to (ii) differences between the value of w where the vortex sheet was shed and at S_x . If both differences (i) and (ii) were absent, then by the condition determining the strength Ξ of the vortex sheet it is the same vortex sheet as that attached to a solid fin, and hence by the uniqueness theorem of hydrodynamics the flows are the same.

For small gaps both differences (i) and (ii) are small. Note that because the body undulation propagates at a speed V not very much greater than U , the value of w at S_x has only a slight phase advance over that obtaining where the vortex sheet was shed, although there may also be a slight amplitude increase at the posterior section. The whole analysis applies to ventral just as much as to dorsal fins, and suggests in either case that with anguilliform motion a succession of closely spaced fins is dynamically equivalent to a long continuous fin, as stated by Lighthill (1969; last sentence of §4).

In certain fishes, by contrast, including most cat-fishes of the sub-order Siluroidea (order Ostariophysi), anguilliform motion is retained although there is a large gap between the main dorsal fin and the caudal fin (any second dorsal fin being relatively insignificant). Analysis of their motion must take into account the extensive region of vortex sheet between the dorsal and caudal fins, where the above-noted differences (i) and (ii) may be sufficiently important to make the sheet behave very differently from a solid fin.

These differences make it necessary to define at each body section S_x a separate virtual mass $\tilde{m}(x)$ per unit length for the vortex sheet in the presence of the body section. To do this, we bear in mind that the velocity potential on the two sides of the vortex sheet has a certain value proportional to

$$w_F = w(x_F, t - (x - x_F)/U), \tag{19}$$

the value of w at the fin's posterior edge $x = x_F$ at the time when water now at S_x was passing that edge. The coefficient of proportionality depends on the fish's cross-sectional shape at $x = x_F$, and is given by (16) with $s = s(x_F)$ in the special case of a fish thin in relation to its depth.

We continue to define $m(x)$ as the virtual mass per unit length associated with the motion in the z -direction of an infinite rigid cylinder C_x with cross-section S_x ,

in the absence of any vortex sheet. For motion of C_x with velocity w relative to the water, the cross-flow potential ϕ is that which satisfies

$$\partial\phi/\partial n = wn_z \quad \text{on } C_x, \quad \phi = 0 \quad \text{on vortex sheet,} \quad (20)$$

where n_z is the z -component of a unit vector normal to S_x . The momentum of the flow is $m(x)w$ per unit length.

On the other hand, we define $\tilde{m}(x)$ as the virtual mass associated with the vortex sheet in the presence of a completely stationary cylinder C_x . The associated potential $\tilde{\phi}$ is that which satisfies

$$\partial\tilde{\phi}/\partial n = 0 \quad \text{on } C_x, \quad \tilde{\phi} = \text{given on vortex sheet,} \quad (21)$$

the given value being proportional to w_F (see equation (19)), and the momentum of the flow is taken to be $\tilde{m}(x)w_F$ per unit length. The complete cross-flow, resulting from the motion of S_x in the presence of the vortex sheet, is defined, evidently, by the potential $\phi + \tilde{\phi}$, and its momentum is therefore

$$m(x)w + \tilde{m}(x)w_F. \quad (22)$$

The kinetic energy of this combined flow also has a simple form, because it follows from Green's theorem that the two cross-flows ϕ and $\tilde{\phi}$ are orthogonal in a space with kinetic energy as norm. (This requires that $\oint \phi(\partial\tilde{\phi}/\partial n) ds$, taken over a contour consisting of C_x and the two sides of the vortex sheet, is zero, which is obvious from equations (20) and (21).) Hence the kinetic energy is

$$\frac{1}{2}m(x)w^2 + \frac{1}{2}\tilde{m}(x)w_F^2. \quad (23)$$

The correctness of these formulas (22) and (23) is easily verified for particular cross-sectional shapes; thus, for a thin cross-section S_x we obtain them by direct calculation with

$$\tilde{m} = \frac{1}{4}\pi(\bar{s}^2 - s^2)\rho, \quad m = \frac{1}{4}\pi s^2\rho, \quad (24)$$

where \bar{s} and s are the local depths of cross-section with and without the vortex sheet included. The formulas (24) make clear that at $x = x_F$ (where the vortex sheet starts) there is no discontinuity between the values of $m(x)$ for $x < x_F$ and of $m(x) + \tilde{m}(x)$ for $x > x_F$. Actually, this is a general property for all shapes of body cross-section, because at $x = x_F$ we have $w = w_F$ by (19) and so by (22) the momentum (which as explained earlier must be continuous) is $[m(x) + \tilde{m}(x)]w$.

We may now apply the above results to the estimate of forces between the body and the water. We can no longer write the sideforce Z as equation (6), but instead (using (19) and (22)) as

$$\begin{aligned} Z &= \left(\frac{\partial}{\partial t} + U \frac{\partial}{\partial x} \right) \left[m(x)w(x, t) + \tilde{m}(x)w \left(x_F, t - \frac{x - x_F}{U} \right) \right] \\ &= \left(\frac{\partial}{\partial t} + U \frac{\partial}{\partial x} \right) [m(x)w(x, t)] + U\tilde{m}'(x)w \left(x_F, t - \frac{x - x_F}{U} \right), \end{aligned} \quad (25)$$

provided that we remember that \tilde{m} jumps practically discontinuously at $x = x_F$ from 0 to $\tilde{m}(x_F)$, so that the $\tilde{m}'(x)$ in (25) includes a delta-function term $\tilde{m}(x_F)\delta(x - x_F)$, while according to the previous paragraph $m'(x)$ includes an equal and opposite delta-function term.

Equation (7) for the rate E at which the fish is doing work through its transverse movements with velocity $\partial h/\partial t$, exerting forces Z per unit length, can now be transformed into a form similar to (8) but with an interesting extra term. The first term on the right of (25) gives precisely the terms on the right of (8), the argument being unmodified by the fact that $m(x)$ is discontinuous at $x = x_F$. The term in $\tilde{m}'(x)$ on the right of (25), on the other hand, contributes two terms to (7), one from the delta function and one from the remainder of $\tilde{m}'(x)$, so that we have

$$\begin{aligned}
 E = \frac{\partial}{\partial t} \int_0^l \left(mw \frac{\partial h}{\partial t} - \frac{1}{2} mw^2 \right) dx + U \left[mw \frac{\partial h}{\partial t} \right]_{x=l} \\
 + U \tilde{m}(x_F) w(x_F, t) \frac{\partial}{\partial t} h(x_F, t) \\
 + \int_{x_F}^l U \tilde{m}'(x) w \left(x_F, t - \frac{x - x_F}{U} \right) \frac{\partial}{\partial t} h(x, t) dx. \quad (26)
 \end{aligned}$$

The other method (10) of writing E , from which the thrust P can be obtained by subtraction, calculates rates of change of energy in the frame of reference in which the undisturbed water is at rest. With the modified form (32) of the kinetic energy per unit length, it becomes

$$E = UP + U \left[\frac{1}{2} mw^2 + \frac{1}{2} \tilde{m} w_F^2 \right]_{x=l} + \frac{\partial}{\partial t} \int_0^l \left(\frac{1}{2} mw^2 + \frac{1}{2} \tilde{m} w_F^2 \right) dx. \quad (27)$$

The fishes with which we are here concerned have the depth of their caudal fin practically as large as (or larger than) that of the dorsal fin and body combined. These, then, are fishes which reabsorb the vortex sheet from the dorsal fin on to the caudal fin, where it gets mixed with the boundary layer, so that the vortex sheet finally shed from the caudal fin, being determined by that fin's motion relative to the water, is practically uninfluenced by the incident sheet. At the trailing edge $x = l$, then, no separate vortex sheet from the dorsal fin remains, which means that $\tilde{m} = 0$ and that the second term on the right of (27) takes the same form as in (10); in other words, rate of shedding of kinetic energy of water motions into the wake is unaffected by the vortex sheet in the gap between the dorsal and caudal fins.

Admittedly, the last term on the right of (27) is modified by this vortex sheet, but this is still the rate of change of a fluctuating quantity and so has mean value zero. Hence the mean rate of wastage of energy $\bar{E} - UP$ is unaffected, according to the approximations here used, by the vortex sheet in the gap. This makes it particularly interesting to enquire whether the total mean rate of working \bar{E} given by (26) can be increased by the new vortex-sheet terms, because if so then all the extra power should be effective propulsively and the fish should achieve simultaneous improvements in thrust and efficiency.

This does in fact seem to be possible, and for reasons which can be given a clear physical interpretation. The first term in (26) has zero mean, and the second is the usual $UmwW$ term, interpreted earlier as rate of shedding of lateral momentum from the caudal fin times trailing-edge lateral velocity. This term can, as we know, have a positive mean. The third term has an identical interpretation in relation to

the dorsal fin and can for the same reason (essentially because $V > U$) have a positive mean.

We must ask therefore whether the last term in (26), in which the factor $\tilde{m}'(x)$ must on the average be negative as \tilde{m} decreases from the positive value $\tilde{m}(x_F)$ to the zero value $\tilde{m}(l)$, must necessarily cancel the third term in mean value. Certainly we can interpret this last term as a negative rate of working, equal to minus an integral over the caudal fin's leading edge of the product of its rate of picking up of lateral momentum from the vortex sheet, $U(-d\tilde{m})w_F$, with the lateral velocity of the caudal-fin leading edge $\partial h/\partial t$. That term is actually negative however only if the quantity $w_F \partial h/\partial t$ occurring in it possesses a positive mean value.

This might be thought inevitable if $V > U$, and the mean value in question might be supposed greater even than the value at the dorsal-fin trailing edge, because of posterior increase in amplitude. This is not necessarily true, however, if there is a substantial phase difference between w_F and $\partial h/\partial t$ at the caudal-fin leading edge. If this phase difference exceeds $\frac{1}{2}\pi$, their mean product might be negative.

In terms of a mean position $x = x_C$ of the caudal-fin leading edge, this phase difference has a mean value

$$\frac{2\pi(x_C - x_F)}{\lambda} \left(\frac{V}{U} - 1 \right), \quad (28)$$

where λ is the wavelength of the undulation. This is because $2\pi(x_C - x_F)/\lambda$ is the phase difference in $\partial h/\partial t$ between $x = x_F$ and x_C , while the phase difference in w_F , as (19) shows, is greater by a factor V/U owing to vorticity convection at a speed U slower than the speed V of the body undulation. With a gap $(x_C - x_F)$ of at least half a wavelength, as is common, and typical values of U/V around $\frac{2}{3}$, the phase difference (28) can well be $\frac{1}{2}\pi$ or more.

The above argument seems to indicate that a large enough gap between the dorsal and caudal fins can improve the anguilliform mode by increasing total power output without any increase in the power wasted in creating a vortex wake. This is because momentum shedding from the dorsal fin, in phase with its lateral motion, causes mean power to be exerted but the rate of annihilation of that momentum, after it has reached the caudal fin at a speed U less than the propagation speed V of the body undulation, is out of phase (or is even in antiphase) with the caudal fin's lateral velocity, and so does not produce any balancing reduction in power output.

It is conceivable that the arguments of this section might have some bearing on the problem of the evolution of discrete dorsal fins. Primitive jawless vertebrates of the class Cyclostomata, such as lampreys and hagfishes, possess continuous dorsal fins. We have suggested that their replacement at some stage of fish evolution by a sequence of closely spaced discrete fins would not be disadvantageous as regards thrust, while its effect on drag reduction might be beneficial. Later on, reinforcement of the first dorsal fin and reduction of the others might be favoured by additional (phase-related) considerations of thrust advantage in the first place, although advantages relating to stability and control in yaw would soon emerge.

4. Mechanics of the carangiform mode

Still later, further improvements in thrust and efficiency might result from gradual conversion to the carangiform mode, in which the dorsal fin no longer sheds a vortex sheet, playing a different, although still essential, role. Mechanical considerations relating to this further development must now be set out. We shall see that the confinement of undulations to a reduced fraction of the fish's length in the neighbourhood of the caudal fin produces a gain in efficiency, which however might well have been cancelled out by losses due to 'recoil' effects if adoption of carangiform motion had not been accompanied by morphological changes tending to minimize these.

To understand the gain, we must further refine the theoretical considerations of §2 by taking into account the fact (noted already in the paragraph following equation (3)) that pushing a slice of water with a body of virtual mass m gives the water not only an immediate access of momentum mw but also a subsequent gradual further increase of momentum. This is associated with the vortex-force on the body, which is a direct result of vorticity progressively shed by the body as the pushing continues. At the same time the water's kinetic energy increases above the energy $\frac{1}{2}mw^2$ of the irrotational flow (by an amount equal, as Kelvin's 'minimum energy theorem' shows, to the energy that the vortex system would possess with the body stationary).

Lighthill (1960) suggested very tentatively that the theory of §2 could be extended as follows to take into account changes (if they could be estimated) in the water's momentum M and kinetic energy T per unit length from the values mw and $\frac{1}{2}mw^2$. Note that various checks made on equations (9) and (10) in §2 suggest that the physical ideas leading directly to those equations may possibly be reliable in more general cases. If these are used to predict only mean values \bar{P} and \bar{E} of thrust and rate of working, they yield

$$\bar{E} = U[\overline{MW}]_{x=l}, \tag{29}$$

$$\bar{E} - U\bar{P} = U[\overline{T}]_{x=l}, \tag{30}$$

the differences being in each case the mean value of a rate of change of kinetic energy of the water motions adjacent to the body, in a frame of reference in which either the body, or the water respectively, is at rest. Such kinetic energy immediately adjacent to the body in each case fluctuates periodically, so that its time rate of change has mean value zero.

For mean thrust and efficiency, equations (29) and (30) imply

$$\bar{P} = [\overline{MW} - \overline{T}]_{x=l} = \{V/(V-U)\} \overline{Mw} - \overline{T}_{x=l}, \tag{31}$$

$$\eta = 1 - \{(V-U)/V\} [\overline{T}]_{x=l} / [\overline{Mw}]_{x=l}, \tag{32}$$

equations in which equation (3) is still used to express W in terms of w . These suggest that parts of the momentum M at the trailing edge $x = l$ which are badly correlated with the local pushing velocity w may be ineffective for producing thrust, while the associated parts of the kinetic energy T might add very considerably to the wasted energy in the vortex wake.

The momentum per unit length of fish, M , in a water slice normal to that length that has just reached the trailing edge, has been changed from the virtual-mass value mw by an amount equal to the vortex-force applied by different sections of the fish which it passed, integrated with respect to time. Unfortunately, it is impossible to attempt an accurate estimate of vortex-force on the water slice in the exceedingly unsteady conditions while it is pushed at varying velocities by cross-sections of varying shapes, and it is even harder to estimate the addition to $\frac{1}{2}mw^2$ at the trailing edge, namely the local value of the vortex-system energy. However, very crude estimates suffice to make plausible the substantial reduction in efficiency of anguilliform motion through these effects, and the virtual disappearance of such reduction resulting from a modification into carangiform motion.

The crude estimate used here, for vortex-force per unit length due to pushing at velocity w , is based on two simplifying approximations. First, a drag depending only on w and on the cross-sectional depth s , and characteristic of steady motion of a long thin strip at right angles to its plane (Flachsbart 1935) is used; this is $\rho sw^2 \operatorname{sgn} w$, where the $\operatorname{sgn} w$ ($+1$ if $w > 0$ and -1 if $w < 0$) expresses that the drag force is in the same direction as the velocity. Secondly, an approximate linearization of this is used. If w varies between $-w_0$ and $+w_0$, then the r.m.s. absolute error in replacing $w^2 \operatorname{sgn} w$ by the regression line $\frac{3}{4}w_0 w$ is only $0.11w_0^2$. This linearization is reasonable in the present context where drags at different velocities contribute linearly to the total momentum M (so that only absolute errors, not the relative errors which are far bigger for small w , are relevant).

This leads to the value $\frac{3}{4}\rho sw_0 w$ for vortex-force, which used together with the virtual-mass contribution to momentum is like representing the water reaction to motion of fish cross-sections as a combination of a linear resistance and an inertance. The excessive momentum at the trailing edge $x = l$ at time t is now represented as an integral with respect to time t_1 of a vortex-force proportional to the value at that time of the product sw at the point $x = l - U(t - t_1)$ where the water slice then was:

$$\begin{aligned} [M]_{x=l} &= [mw]_{x=l} + \int_{t-U}^t \frac{3}{4}\rho w_0 [sw(l - U(t - t_1), t_1)] dt \\ &= [mw]_{x=l} + \int_0^l \frac{3}{4}\rho w_0 [sw(x, t - (l - x)U^{-1})] dx/U. \end{aligned} \quad (33)$$

We can compare the phase relationships between M and w at $x = l$ for different rates of growth of wave amplitude with x by evaluating (33) with

$$sw(x, t) = s_0 w_0 e^{\kappa(x-l)} \cos [\omega(t + (l - x)V^{-1})], \quad (34)$$

where V is the wave speed relative to the body and κ is small for anguilliform motion but large for carangiform. If m is approximately represented (see §2) as $\frac{3}{4}\rho s^2$ this gives

$$[M]_{x=l} = \frac{3}{4}\rho s_0^2 w_0 \cos \omega t + \frac{\frac{3}{4}\rho s_0 w_0^2 [\kappa \cos \omega t + \omega(U^{-1} - V^{-1}) \sin \omega t]}{U[\kappa^2 + \omega^2(U^{-1} - V^{-1})^2]}, \quad (35)$$

where the small contribution to the integral in (33) from the lower limit has been neglected. Hence

$$[\overline{Mw}]_{x=l} = \frac{3}{8}\rho s_0^2 w_0^2 + \frac{\frac{3}{8}\rho s_0 w_0^3 \kappa}{U[\kappa^2 + \omega^2(U^{-1} - V^{-1})^2]}. \quad (36)$$

These results show that for small κ the phase lag relative to $[w]_{x=l}$ in the part of $[M]_{x=l}$ due to momentum gain from anterior sections reduces considerably the value (36) of their mean product. The value of $[T]_{x=l}$ is not so affected. The part due to vortex-force can be estimated as an integral with respect to time t_1 of w times the vortex-force, giving

$$[T]_{x=l} = [\frac{1}{2}mw^2]_{x=l} + \int_0^l \frac{3}{4}\rho w_0[sw^2(x, t - (l-x)U^{-1})]dx/U. \quad (37)$$

Now taking $sw^2(x, t) = s_0 w_0^2 e^{\tau(x-l)} \cos^2 [\omega(t + (l-x)V^{-1})]$, (38)

which with s taking its maximum value s_0 at the trailing edge implies $\kappa \leq \tau \leq 2\kappa$, equation (37) becomes

$$[\bar{T}]_{x=l} = \frac{3}{16}\rho s_0^2 w_0^2 + \frac{3}{8}\rho s_0 w_0^3 U^{-1}\tau^{-1}. \quad (39)$$

We conclude from (39) that the energy flow into ‘wasted’ wake motions is increased through vortex-force effects on body cross-sections by a factor about $1 + 2w_0/U\tau s_0$. Here $2w_0/U$ is of order 1 for a wide range of fish motions, so the increase in wasted energy is significant if τ is of order of magnitude around s_0^{-1} or less, as in anguilliform motion. This increase is not balanced by a corresponding increase of thrust because for such values of τ (and corresponding values of κ down to one-half as much) (36) shows $[\bar{M}w]_{x=l}$ to be insignificantly increased† essentially because the addition to $[M]_{x=l}$ is poorly correlated with $[w]_{x=l}$, when, as is normal, the term $\omega(U^{-1} - V^{-1})$ in (36) is itself of order s_0^{-1} .

For carangiform motion, on the other hand, there is a rapid increase of amplitude of motions near the caudal fin, and τ , the relative rate of increase of sw^2 , is significantly larger than s_0^{-1} , generating a far smaller increase in wasted energy. Thus, carangiform motion represents the logical dénouement of the process begun by posterior lateral compression. The utilization of the virtual-mass effect (the water’s ‘inertance’ as opposed to its ‘resistance’), which lateral compression made possible, becomes in carangiform motion almost the exclusive basis of thrust production.

With the transition to carangiform motion, however, there arises a possibility of one other source of thrust reduction through imperfect correlation of $[M]_{x=l}$ and $[W]_{x=l}$, namely the ‘recoil’ effect (Lighthill 1960). This can lead to additional vortex-force, and also to a possible departure from equation (3), which states that W and w are perfectly in phase; such departure may decrease the rate of working, and reduction in the ratio of their amplitudes may at the same time increase wasted energy. The derivation of that equation, and others, assumed that a fish can by muscular action cause a wave of lateral movement specified by some definite equation for $h(x, t)$ to pass down its body. This ignores the fact that the lateral movement of the fish is subject to two overriding laws of motion:

† The estimate (36) for $\bar{E}(V-U)/VU$ is based on the tentative equation (29), which may overestimate the extent to which the effect of vortex-force wakes is modified by posterior motions. However, an opposite assumption, that the increase in \bar{E} due to vortex-forces is exactly equal to the extra work that they locally do through pushing at velocity W , would replace the second term in (36), as an equation for $\bar{E}(V-U)/VU$, by $\frac{3}{8}\rho S_0 w_0^3 U^{-1}\tau^{-1}$, and the relative increase in work done would still be only half as much as the relative increase in wasted energy.

(i) the rate of change of lateral momentum of the fish must equal the total sideforce with which the water acts on it; (ii) the rate of change of its angular momentum about a fixed axis (which we take as the axis $x = l, z = 0$) must equal the moment of the sideforces with which the water acts on it.

Actually the fish's muscular contractions can only determine changes in its shape relative to the centre of gravity; at the same time, translations and rotations of that shape must in general accompany those changes, and must be such that conditions (i) and (ii) above are satisfied. For example, an attempt to generate an undular lateral displacement

$$h = H(x) \cos [\omega(t + (l-x) V^{-1})] \quad (40)$$

will in practice generate the displacement

$$h = H(x) \cos [\omega(t + (l-x) V^{-1})] + [h_1 + h_3(l-x)] \cos \omega t + [h_2 + h_4(l-x)] \sin \omega t, \quad (41)$$

where the constants h_1, h_2, h_3 and h_4 must be determined by applying conditions (i) and (ii) above and equating the coefficients of $\cos \omega t$ and $\sin \omega t$ on both sides.

We carry out this calculation, with vortex-force neglected, as follows. We first obtain the 'net' total sideforce (by 'net' we mean after correction for rate of change of the fish's own momentum) associated with the simple motion (40), say

$$\int_0^l (Z + m_f \partial^2 h / \partial t^2) dx = Z_1 \cos \omega t + Z_2 \sin \omega t, \quad (42)$$

where $m_f(x)$ is fish mass per unit length, and the 'net' moment of sideforces about the line $x = l, z = 0$ (which is the undisturbed position of the trailing edge),

$$\int_0^l (l-x) (Z + m_f \partial^2 h / \partial t^2) dx = Z_3 \cos \omega t + Z_4 \sin \omega t. \quad (43)$$

Then we find what full expression of the form (41) would make such additions to both the total sideforce and the moment of sideforces that conditions (i) and (ii) would be satisfied. This requires the linear terms in (41) to be such that the integrals in (42) and (43) when calculated for them alone take the same values but with the sign changed.

The calculation is done in two parts like this because different terms are dominant in the quantitative expressions for elements in (42) and (43) which arise from the sinusoidal term (40) in h and from the linear terms added to h in (41). For example, the sinusoidal term in carangiform motion (with $H(x)$ significant only rather near $x = l$) produces a negligible fish-mass element in (42) and (43), because posterior lateral compression makes fish mass negligible compared with virtual mass of water near $x = l$, while corresponding virtual-mass elements, on the other hand, are dominated by the tendency, expressed in equation (3), for values of w associated with this term to be considerably smaller than corresponding values of W .

By contrast, the linear terms in (41) produce fish-mass elements in (42) and (43) that involve the fish's whole inertia, as well as its first and second moments about $x = l$. Furthermore, for these linear terms the $U \partial / \partial x$ parts in (2) and (6) are not nearly so important as the $\partial / \partial t$ parts for the actual frequencies ω that are used (with $\omega l / U$ of order 10). As a first crude approximation, neglecting the $U \partial / \partial x$ parts, those equations give $Z = m(x) \partial^2 h / \partial t^2$, so that the integrals in (42) and (43)

can be calculated as for a rigid body subject to no external forces whose mass distribution is $m(x) + m_f(x)$ per unit length.

This first crude approximation, that the fish's recoil to given sideforces takes the form of an inertial response based on the combined inertia of the fish and the water, is quite a useful one. In terms of

$$M = \int_0^l (m + m_f) dx, \quad ML = \int_0^l (l - x) (m + m_f) dx, \quad I = \int_0^l (l - x)^2 (m + m_f) dx, \tag{44}$$

where L is distance of the centre of inertia from the trailing edge, and $I - ML^2$ is the moment of inertia about that centre of inertia, it gives

$$\begin{pmatrix} M\omega^2 & ML\omega^2 \\ ML\omega^2 & I\omega^2 \end{pmatrix} \begin{pmatrix} h_1 + ih_2 \\ h_3 + ih_4 \end{pmatrix} = \begin{pmatrix} Z_1 + iZ_2 \\ Z_3 + iZ_4 \end{pmatrix}, \tag{45}$$

with the simple solution

$$\frac{[(I/M)Z_1 - LZ_3, (I/M)Z_2 - LZ_4, Z_3 - LZ_1, Z_4 - LZ_2]}{\omega^2(I - ML^2)} \tag{46}$$

for $[h_1, h_2, h_3, h_4]$. The exact form of the matrix that should appear on the left-hand side of (45) can, actually, be calculated as

$$\begin{pmatrix} M\omega^2 + m(l)Ui\omega & ML\omega^2 - M_wUi\omega + m(l)U^2 \\ ML\omega^2 + M_wUi\omega & I\omega^2 + M_wU^2 \end{pmatrix}, \tag{47}$$

where $M_w = \int_0^l m dx$ is the total virtual mass (inertia of the water alone for lateral rigid-fish movements), and the departures of the associated exact solutions from those in (46) are not great.

These considerations on recoil are potentially rather important for carangiform motion (with $H(x)$ in (40) significant only in a short posterior portion of the fish) because the associated total sideforce (42) is potentially rather large. By equation (2), the w associated with (40) is

$$w = UH'(x) \cos[\omega(t + (l - x)V^{-1})] - (V - U)V^{-1}H(x)\omega \sin[\omega(t + (l - x)V^{-1})]. \tag{48}$$

This formula emphasizes the fact that the small value of w relative to W implied by equation (3) is confined to that small region near the trailing edge where the amplitude $H(x)$ of undulation has reached a plateau with $H'(x)$ negligible. Much greater values of w are to be expected in the anterior region where $H(x)$ is rapidly increasing.

If the virtual mass $m(x)$ continues in this region to take large values (such as were shown in § 2 to be necessary at the trailing edge itself) then the fluid momentum $m(x)w(x, t)$ rises to large peak values, and so the associated sideforces (6) are very big. In fact, their total integrated value

$$\int_0^l Z dx = \frac{\partial}{\partial t} \int_0^l mw dx + [Umw]_{x=l} \tag{49}$$

consists of two terms, one associated with fluctuations in the lateral momentum of water movements anterior to the trailing edge, and one associated with

momentum being transferred to the wake. The latter is important in relation to mean rate of working (§2), but the former constitutes a much bigger fluctuating sideforce when mw possesses a large peak.

If the rapid rise of $H(x)$ from 0 to its trailing-edge value $H(l)$ is centred around $x = x_r$, where m takes values that are not depressed to compensate for that rapid rise, then a rough estimate of (49) in which the integral is estimated solely by the contribution from the rise, taken as instantaneous, is

$$\int_0^l Z dx = -Um(x_r)H(l)\omega \sin[\omega(t + (l - x_r)V^{-1})] - Um(l)H(l)(V - U)V^{-1}\omega \sin \omega t. \quad (50)$$

The two terms differ only moderately in phase, and the first term greatly augments the whole through its lack of the $(V - U)V^{-1}$ factor. Similar augmentation is absent with anguilliform motion, where spatial variation of the cosine term in (48) greatly reduces the fluctuations in the integral (49).

It is clear from these considerations that, unless the adoption of carangiform motion is accompanied by a substantial reduction of cross-section depth (with associated large reduction in $m(x)$, as (4) shows) in the neighbourhood of $x = x_r$, where the rapid rise in wave amplitude occurs, total sideforce will be large. Under those circumstances, recoil amplitudes will also be large, as equation (46) implies. Actually the Z_1 and Z_2 terms are the important ones there, and the moment of sideforce about $x = l$ is less important (because the effective action of the sideforce is near $x = l$). The lateral recoil is roughly obtained, therefore, by multiplying (50) by

$$I/[M(I - ML^2)\omega^2]. \quad (51)$$

Here $I - ML^2$ is the moment of inertia of fish plus water around its centre of inertia and can be written Mk^2 , where k is a radius of gyration and can be expected to be substantially less than L . The recoil amplitude associated with the first term in the total sideforce (50) would therefore be

$$[(L^2 + k^2)/k^2][m(x_r)l/M](U/\omega)H(l), \quad (52)$$

which is a by no means negligible fraction of $H(l)$ itself. Although the U/ω factor is of order 10^{-1} , the factor $(L^2 + k^2)/k^2$ can easily be of order 4 or 5, and the factor $m(x_r)l/M$ is of order 1 unless $m(x_r)$ is artificially reduced.

Substantial angular recoil (given by h_3 and h_4) is also produced, and large lateral motions are generated all along the length of the fish. This wipes out the whole potential advantage of carangiform motion, namely its confinement of lateral motion to a short posterior portion. Water arriving at the trailing edge has been subjected to vortex drag, not just while it traversed such a short posterior portion, but for a much longer time, and has acquired additional vortex motions with substantial energy whose momentum is badly correlated with the trailing-edge velocity (both results being harmful, by (29) and (30)).

Accordingly, it is not surprising that the adoption of carangiform motion goes together (Lighthill 1969) with a large reduction of depth of body and fin in the region of abrupt amplitude increase. Then near $x = x_r$, the virtual mass $m(x)$ is so small that there is no peak in lateral momentum, and hence no associated large sideforces.

Some sideforce still remains, however; smaller, admittedly, owing to the $(V - U) V^{-1}$ factor in the second term of (50), but still capable of producing observable recoil, since $m(l)$ must be large for adequate thrust production. It is most important, therefore, that the multiplying factor (51) is kept small, so that the residual sideforce does not generate too much recoil. This requires a large fish depth in an extensive length of the anterior part of the fish.

To see this, suppose that the caudal-fin shape were specified (primarily by thrust considerations) and had total inertia M_C , and consider different specifications for the anterior portion of fish, with total inertia M_A , and centre of inertia at $x = l - l_A$, about which its moment of inertia is $M_A k_A^2$. Then $M = M_A + M_C$, and approximately $ML = M_A l_A$, $I = M_A (l_A^2 + k_A^2)$. It follows that the multiplying factor (51) can be written

$$\omega^{-2} [M_C + M_A k_A^2 / (l_A^2 + k_A^2)]^{-1}. \tag{53}$$

For this to be small requires above all (since k_A^2 is necessarily a good deal smaller than l_A^2) that the part of the fish anterior to the caudal fin possess a large moment of inertia $M_A k_A^2$ about its centre of inertia, taking inertia of both fish and water into account.

Morphologically, this means that for efficient carangiform motion a fish needs a long anterior section of body with its mass so disposed that a large virtual mass of water is drawn into participation in its lateral movements. A degree of lateral compression now becomes advantageous in the anterior part of the fish. Additionally, a large overall depth s between dorsal and ventral fin is most valuable for increasing $m(x)$ (in proportion, by equation (4), to s^2), and the greater the proportion of the fish's length in which such an increased depth is found the more effectively is the recoil reduced.

Among the disadvantages of recoil, the above discussion has emphasized the associated vortex-force losses, but any substantial recoil would also bring other difficulties. At $x = l$, the full equation (41) implies that

$$W = \partial h / \partial t = -\omega [H(l) + h_1] \sin \omega t + \omega h_2 \cos \omega t, \tag{54}$$

and the equations for the recoil coefficients show that h_1 is negative, which reduces the amplitude of W at the trailing edge (for given fish deformations) and so tends to reduce the mean thrust

$$\bar{P} = [m(\overline{wW} - \frac{1}{2}\overline{w^2})]_{x=l}. \tag{55}$$

(Specifically, equation (50) or any other estimate of (49) shows not only that Z_2 is large and negative, but also that Z_1 , the coefficient of $\cos \omega t$, is negative; the moments (43) are smaller but it turns out that Z_3 is positive, and both results combine in (46) to make h_1 (as well as h_2) negative. If the more exact matrix (47) is used, the phase of $h_1 + ih_2$ is reduced slightly, which makes h_1 still more negative.)

Next, the perfect correlation between w and W expressed by equation (3) is in general destroyed at the trailing edge by recoil effects, with harmful effects on the mean thrust (55) and on the efficiency (12). At $x = l$, equations (2) and (41) give

$$w = -[\omega(V - U) V^{-1}H(l) + \omega h_1 + U h_4] \sin \omega t + [UH'(l) + \omega h_2 - U h_3] \cos \omega t. \tag{56}$$

In the absence of recoil it is important that $H'(l)$ be negligibly small in (56) (i.e. that just before the trailing edge wave amplitude cease to increase fast) so that w and W are well correlated. However, if $H'(l)$ is negligible, then recoil (which makes both ωh_2 and $-Uh_3$ negative) produces a greater coefficient of $\cos \omega t$ in w than in W , with harmful effects on the efficiency (12). Further, adoption of a positive value of $H'(l)$ such that the recoil coefficients just made the coefficient of $\cos \omega t$ in (56) small and negative (to restore the correlation with W) might involve too fine an adjustment to be useful as a practical way of getting good efficiency.

To sum up, it is not surprising that fishes adopting carangiform motion possess features suitable for diminishing recoil—particularly, a greatly reduced depth of body in the region immediately anterior to the caudal fin where wave amplitude is increasing rapidly, and, farther forward still, a long region characterized by greatly augmented depth.

5. Two-dimensional theory of the lunate tail

It is possible to trace, from the hydromechanical point of view, three distinct stages in the further development of carangiform propulsion in teleosts (bony fishes), aimed at improving speed and efficiency. First, there is the 'scooping out' of a central posterior portion of the caudal fin (as in the herring *Clupea*) so that the fin becomes geometrically like a pair of highly sweptback wings. Provided that the posterior part of the caudal fin is moving as a rigid whole, the discussion at the beginning of §3 above suggests that no thrust would be lost by this modification, because the vortex-sheet strength in the gap would be the same as its strength on solid parts of fin. The decline in surface area, on the other hand, could produce some slight reduction of resistance and associated gain in speed.

Secondly, there is the reduction of sweepback of the two wing-like surfaces then composing the caudal fin (as in the horse-mackerel *Caranx*). This increases trailing-edge span s (with important thrust benefits, by (4) and (55)), without increasing surface area, and a still greater speed improvement should result. Where, as with *Caranx*, the degree of sweepback can be varied by muscular action, the animal acquires a valuable extra measure of control.

At some point during the process of decreasing sweepback, the elongated-body theory of §§2–4 becomes inapplicable, as explained in §1. Certainly, it is out of the question to apply it to the third type stage of development of carangiform propulsion, when the caudal fin acquires high aspect-ratio s^2/S (where S is its surface area) and the 'lunate' form described in the introduction. This seems to be some sort of culminating point of the process of improvement of speed and efficiency in the teleosts, a supposition that is borne out by the fact that a similar lunate tail was acquired by the fastest sharks and by the cetacean mammals (as well as by *Ichthyosaurus*) through quite different evolutionary processes.

Without discussing these pathways of convergent evolution further, the rest of this section is devoted to a first approximate theory of the carangiform motion of animals with lunate tails. For reasons described in §1, such a first

approximate theory must be a two-dimensional theory, in which the caudal fin (in the case of the fishes) is considered to act independently on each separate horizontal slice of water. This theory must overestimate efficiency because it takes into account only the cross-stream elements of wake vorticity. Here it is set out, however, in a form designed to facilitate later extension to a lifting-line theory that would also take streamwise wake vorticity into account.

In the two-dimensional theory, the section of the caudal fin (in its symmetrical, undisturbed position) by a horizontal water slice $y = \text{constant}$ is taken as stretching from $x = -a$ to $x = +a$ (so that the origin of x is shifted to the half-chord position), and the undisturbed fluid flow has velocity U . The section's lateral displacement is taken as

$$z = [h - i\alpha(x - b)] e^{i\omega t}, \tag{57}$$

where h and α are real numbers signifying the amplitude of the sideslip and yawing motions respectively, and $x = b, z = 0$ is the yawing axis. A 90° phase difference between the sideslip and yawing motions is assumed, but note that any other phase difference, represented by giving an imaginary part to h in (57), is simply equivalent to a change in b .

The velocity potential $\phi e^{i\omega t}$ of flow disturbances satisfies boundary conditions which, on linearization, can be applied on $z = 0$ and take the following form. For $-a < x < a$,

$$(\partial\phi/\partial z)_{z=0} = i(\omega h - U\alpha) + \omega\alpha(x - b), \tag{58}$$

which equates lateral velocity of fluid to the rate of change, $\partial z/\partial t + U \partial z/\partial x$, of the section's lateral displacement (57) relative to a particular water slice. Symmetry shows also that ϕ must be an odd function of z , and this means on $z = 0$ that ϕ vanishes for $x < -a$ (upstream of the leading edge). This argument fails for $x > a$, downstream of the trailing edge, where a vortex sheet must be present for the same reasons as were adduced in §3 (but in this two-dimensional flow including only cross-stream vorticity). Its strength is unchanging relative to the fluid, so that on $z = 0, x > a$ the quantity

$$\Phi = i\omega\phi + U \partial\phi/\partial x \tag{59}$$

is a continuous as well as an odd function of z and therefore vanishes.

It is convenient, following Possio (1938) and also Wu (1961), to use Φ as a new dependent variable, particularly since it is continuous throughout the fluid and vanishes on $z = 0$ for both $x < -a$ and $x > +a$. Also, it has important physical significance, since departures of the pressure p from its hydrostatic value p_0 take the form

$$p - p_0 = -\rho\Phi e^{i\omega t} \tag{60}$$

on linearized theory, and thus it is the continuity of pressure across the vortex sheet which is essentially being used. For $-a < x < a$, we have by (58) and (59)

$$(\partial\Phi/\partial z)_{z=0} = B + Cx, \quad \text{where } B = 2U\omega\alpha - \omega^2(h + i\alpha b), \quad C = i\omega^2\alpha, \tag{61}$$

an equation which relates lateral pressure gradient to lateral acceleration of a fluid element resulting from the fin's displacement (57).

Solutions of $\nabla^2\Phi = 0$ satisfying (61) are easily obtained, but we must consider carefully what singularities can be permitted, or are necessary, so that such a

solution corresponds to a value of ϕ satisfying the boundary conditions. As in many steady-oscillation problems, it is convenient to think of ω as possessing a small negative imaginary part (which is later allowed to tend to zero), representing a slow build-up of the oscillation to its present level. Then equation (59) can be solved for ϕ as

$$\phi = U^{-1} \int_{-\infty}^x \Phi(x_1, z) e^{i\omega(x_1-x)/U} dx_1, \tag{62}$$

which automatically vanishes for $z = 0, x < -a$ (as it should) if Φ does.

The singularities of ϕ needed to represent flow near the leading and trailing edges are well known. Near a sharp trailing edge $x = a$, where the Kutta-Zhukovskii condition of no flow around the edge is applied, ϕ has a three-halves power singularity (so that $(\phi)_{z=0}$ is of order $(a-x)^{3/2}$). This means that Φ , and the pressure

Φ	Φ_1	Φ_2	Φ_3
$\Omega + i\Phi$	$1 - [(\zeta - a)/(\zeta + a)]^{1/2}$	$\zeta - (\zeta^2 - a^2)^{1/2}$	$\frac{1}{2}\zeta^2 - \frac{1}{2}\zeta(\zeta^2 - a^2)^{1/2}$
$(\Omega)_{z=\pm 0} \begin{cases} x < a \\ x > a \end{cases}$	$\begin{matrix} 1 \\ 1 - [(x-a)/(x+a)]^{1/2} \end{matrix}$	$\begin{matrix} x \\ x - (x^2 - a^2)^{1/2} \operatorname{sgn} x \end{matrix}$	$\begin{matrix} \frac{1}{2}x^2 \\ \frac{1}{2}x^2 - \frac{1}{2} x (x^2 - a^2)^{1/2} \end{matrix}$
$(\Phi)_{z=\pm 0} \begin{cases} x < a \\ x > a \end{cases}$	$\begin{matrix} \mp [(a-x)/(x+a)]^{1/2} \\ 0 \end{matrix}$	$\begin{matrix} \mp (a^2 - x^2)^{1/2} \\ 0 \end{matrix}$	$\begin{matrix} \mp \frac{1}{2}x(a^2 - x^2)^{1/2} \\ 0 \end{matrix}$
$Z = 2 \int_{-a}^a (\Phi)_{z=0} dx$	$2\pi a$	πa^2	0
$Q = 2 \int_{-a}^a (-x) (\Phi)_{z=0} dx$	πa^2	0	$-\frac{1}{8}\pi a^4$

TABLE 1. This specifies the properties of three solutions Φ_1, Φ_2 and Φ_3 of $\nabla^2\Phi = 0$, each tending to zero as $x^2 + z^2 \rightarrow \infty$, and each defined in terms of the behaviour of a function $\Omega + i\Phi$ of $\zeta = x + iz$, regular outside a cut from $\zeta = -a$ to $\zeta = +a$. Here the square roots of $(\zeta - a)/(\zeta + a)$ and $\zeta^2 - a^2$ mean those 'branches' which behave like 1 and ζ respectively for large $|\zeta|$. Square roots of functions of the real variables x mean the positive square roots. Across the cut $z = 0, |x| < a$, Ω is continuous but Φ is discontinuous. At all points

$$\partial\Phi/\partial z = \partial\Omega/\partial x$$

(60), have square-root singularities. The leading edge $x = a$, on the other hand, permits good hydrodynamic performance *only* if it is well rounded so as to permit flow around the edge, and this corresponds to a square-root singularity in ϕ (so that $(\phi)_{z=0}$ is of order $(x+a)^{1/2}$), and an inverse-square-root singularity in Φ . (More accurate analysis places the singularity a short distance behind the leading edge, equal to half the section's radius of curvature (Lighthill 1951), but the calculations placing it at $x = -a$ give a good approximation when overall forces are being calculated.)

Those considerations specify the required solution of $\nabla^2\Phi = 0$ satisfying (61) as

$$\Phi = A\Phi_1 + B\Phi_2 + C\Phi_3 \tag{63}$$

in terms of functions Φ_1, Φ_2 , and Φ_3 specified in table 1. Here the coefficient A

is arbitrary, and the term in Φ_1 must be included to allow for the expected singularities just referred to.

In order to determine A , we must require that the ϕ specified by (62) and (63) satisfies condition (58), just as it was earlier shown to satisfy the other conditions on ϕ . By table 1, this requires, for $|x| < a$, that

$$U^{-1} \int_{-\infty}^{-a} e^{i\omega(x_1-x)|U} \{Aa(x_1+a)^{-1} + Bx_1 + C(x_1^2 - \frac{1}{2}a^2)\} (x_1^2 - a^2)^{-\frac{1}{2}} dx_1 + U^{-1} \int_{-\infty}^x e^{i\omega(x_1-x)|U} (B + Cx_1) dx_1 = i(\omega h - U\alpha) + \omega\alpha(x - b), \quad (64)$$

where values of $\partial\Phi/\partial z$ equal to $\partial\Omega/\partial x$ have been used. The improper integrals are to be interpreted in the generalized-functions sense (Lighthill 1958), or (in other language) in the Abel sense as $x_1 \rightarrow -\infty$ (equivalent to ω having a negative imaginary part that is allowed to tend to zero), and in the Hadamard sense as $x_1 \rightarrow -a$. This is because $\partial\Phi_1/\partial z$ is the x -derivative of a function Ω whose limit as $z \rightarrow 0$ includes the singular term $-[(x-a)/(x+a)]^{\frac{1}{2}}$ for $x < -a$ but not for $-a < x < a$, and so the corresponding term in (64) would be correctly evaluated through integration by parts with the 'infinite' integrated term replaced by zero.

It is easily verified that the part of (64) written on the second line is separately an identity, as could have been predicted since its left-hand side is the $(\partial\phi/\partial z)_{z=0}$ that would correspond to (61) if the latter gave $(\partial\Phi/\partial z)_{z=0}$ for *all* x , and this must be (58) by the way that (61) was derived. Hence the first line of (64) vanishes separately, and after cancelling the $U^{-1}e^{-i\omega|x|U}$ factor this gives a single condition to determine A .

When the integrals have been evaluated as Bessel functions of

$$r = i\sigma, \quad \text{where} \quad \sigma = \omega a/U \quad (65)$$

(and r should be thought of as having a small positive real part), this condition becomes

$$Ar[K_0(r) + K_1(r)] - BaK_1(r) + \frac{1}{2}Ca^2[K_0(r) + 2r^{-1}K_1(r)] = 0. \quad (66)$$

We show the evaluation only in the (doubly improper) case of the coefficient of A , which on the substitution $x_1 = -a \cosh u$ becomes

$$-\int_0^\infty e^{-r \cosh u} (\cosh u - 1)^{-1} du = [e^{-r \cosh u} \coth \frac{1}{2}u]_0^\infty + r \int_0^\infty e^{-r \cosh u} (1 + \cosh u) du, \quad (67)$$

an integration by parts in which the rules mentioned above require the integrated term to be replaced by zero, while the remaining term is $r[K_0(r) + K_1(r)]$. In terms of the Theodorsen function (Garrick 1957),

$$F(\sigma) + iG(\sigma) = K_1(i\sigma)/[K_0(i\sigma) + K_1(i\sigma)], \quad (68)$$

whose values are displayed in figure 3, equation (66) with (62) and (65) gives

$$A = -U\{\omega\alpha(b - \frac{1}{2}a) + i(U\alpha - \omega h)\} (F + iG) + \frac{1}{2}\omega\alpha a. \quad (69)$$

The sideforce (in the z -direction) per unit span, $\rho Z e^{i\omega t}$ say, and the yawing moment per unit span acting about the half-chord position $x = z = 0$ in the positive sense (that is, tending to turn the leading edge in the z -direction), $Q e^{i\omega t}$ say, are given by (60) and (63) and table 1 as

$$Z = 2 \int_{-a}^a (\Phi)_{z=0} dx = 2\pi a A + \pi a^2 B, \tag{70}$$

$$Q = 2 \int_{-a}^a (-x) (\Phi)_{z=0} dx = \pi a^2 A - \frac{1}{3} \pi a^4 C. \tag{71}$$

From these can be deduced the mean rate of working per unit span, $\rho \bar{E}$ say. We use two principles for this: (i) rate of working in combined sideslip and yawing equals sideforce times rate of sideslip of centroid, plus yawing moment about centroid times rate of yaw; (ii) if two quantities are each expressed as the real part of complex exponentials, $a e^{i\omega t}$ and $b e^{i\omega t}$, their mean product is $\frac{1}{2} \Re(a\bar{b})$ where \Re means real part and \bar{b} the complex conjugate of b .

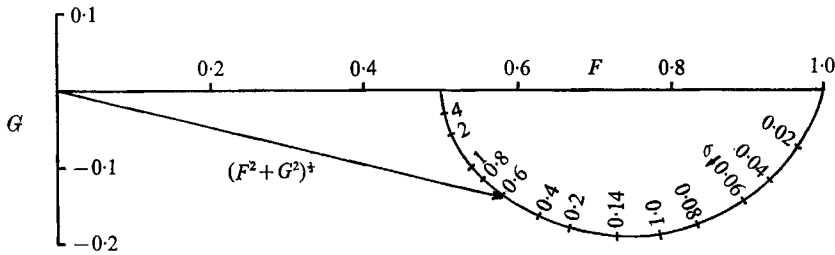


FIGURE 3. Argand-diagram representation, adapted from Garrick (1957), of the Theodorsen function $F + iG$ as a function of the frequency parameter $\sigma = \omega a/U$ (where $a = \frac{1}{2}c$ is the half-chord length of the aerofoil).

These principles give

$$\bar{E} = \frac{1}{2} \Re[Z\omega(-\alpha b - ih) + Q(-\omega\alpha)], \tag{72}$$

since (57) implies a rate of sideslip of centroid $\omega(-\alpha b + ih) e^{i\omega t}$ and a rate of yaw $-\omega\alpha e^{i\omega t}$. From equations (70), (71) and (72), with (61), we obtain

$$\bar{E} = -\pi a \omega \alpha (b + \frac{1}{2}a) \Re A + \pi a \omega h \Im A - \pi a^2 U \omega^2 \alpha^2 b, \tag{73}$$

where \Im means imaginary part.

The mean thrust per unit span is $\rho \bar{P}$, where

$$\bar{P} = \pi a U^{-2} |A|^2 + (\pi a \alpha \Im A - \frac{1}{2} \pi a^2 \omega^2 \alpha^2 b). \tag{74}$$

The term in parentheses here represents the mean resultant $\frac{1}{2} \Re[Z(-i\alpha)]$ of a sideforce $\rho Z e^{i\omega t}$ given by (70) acting on a surface (57) inclined backwards at an angle $i\alpha e^{i\omega t}$ to the x -axis. An important additional thrust, however, is derived from the first term, representing the mean suction force acting on the rounded leading edge due to the fast flow around it. Instantaneously, the suction force takes the well-known steady-flow value obtained by Blasius's theorem (see, for example, Robinson & Laurmann 1956, p. 126). This is associated only with the quadratic terms $-\frac{1}{2} \rho [\partial\phi/\partial x]^2 + (\partial\phi/\partial z)^2$ in the pressure (because the linear

term (60), being an odd function of z , has zero resultant), and the mean suction force is $\frac{1}{2}\pi|K|^2$, where $K(x+a)^{-\frac{1}{2}}$ is the asymptotic form as $x \downarrow -a$ of $(\partial\phi/\partial x)_{z=+0}$, which by (59) is that of $U^{-1}\Phi$ (since ϕ vanishes at $x = -a, z = 0$). Equation (74) follows since this K , by (63) and table 1, is $-U^{-1}A(2a)^{\frac{1}{2}}$.

The rate of energy wastage per unit span, $\rho(\bar{E} - U\bar{P})$, is deduced from (73) and (74) by simple algebra, using (69), as

$$\bar{E} - U\bar{P} = (U\pi a) [\omega^2\alpha^2(b - \frac{1}{2}a)^2 + (\omega h - U\alpha)^2] (F - F^2 - G^2). \tag{75}$$

In this important formula all three factors are essentially positive, and the middle factor shows a clear minimum as a function of b when the yawing axis $x = b$ is at the three-quarter-chord point $b = \frac{1}{2}a$.

More arduously, the formula (75) can be derived by showing that in the region of the vortex wake $x > a$ equations (62) and (63), together with a variety of Bessel-function identities, imply that $(\phi)_{z=\pm 0} = \mp \phi_w e^{-i\omega x/U}$, where

$$\phi_w = \frac{\pi U [\omega h - U\alpha + i\omega\alpha(b - \frac{1}{2}a)]}{\omega [K_0(i\sigma) + K_1(i\sigma)]}. \tag{76}$$

The parts of such a vortex wake far beyond the influence of the solid body $|x| < a$ have mean energy $\frac{1}{2}\rho(\omega/U)|\phi_w|^2$ per unit length, and such energy increases at a rate $\frac{1}{2}\rho\omega|\phi_w|^2$. Agreement of this rate of energy wastage with (75) is then proved by another Bessel-function identity,

$$|K_0(i\sigma) + K_1(i\sigma)|^{-2} = (2\omega a/\pi U) (F - F^2 - G^2). \tag{77}$$

This much more complicated method is only useful as a check.

The efficiency η is still given by equation (1), although in this section both \bar{E} and \bar{P} are values per unit span, divided by the density. Hence, by (69), (73) and (75),

$$\begin{aligned} 1 - \eta &= (\bar{E} - U\bar{P})/\bar{E} \\ &= \frac{\{\omega^2\alpha^2(b - \frac{1}{2}a)^2 + (\omega h - U\alpha)^2\} (F - F^2 - G^2)}{\{\omega\alpha(b - \frac{1}{2}a) [\alpha(b + \frac{1}{2}a)F - hG - \frac{1}{2}\alpha a] + (\omega h - U\alpha) [hF + \alpha(b + \frac{1}{2}a)G]\} \omega}. \end{aligned} \tag{78}$$

The numerator of (78), proportional to the rate of energy wastage, shows the clear minimum as a function of b where $b = \frac{1}{2}a$ already referred to. This minimum is particularly sharp for the higher values of both the frequency parameter $\sigma = \omega a/U$ and the proportional-feathering parameter $U\alpha/\omega h$, which Lighthill (1969) called θ (and which must be expected to be less than 1 for significant positive thrust).

The corresponding maximum in η is shifted to a value of b only slightly greater than $\frac{1}{2}a$ by the behaviour of the denominator. There, the terms in square brackets that form the coefficients of $\omega\alpha(b - \frac{1}{2}a)$ and $(\omega h - U\alpha)$ are both positive near $b = \frac{1}{2}a$, so that total work done increases as $(b - \frac{1}{2}a)$ increases. However, the first of these coefficients is considerably the smaller in most cases of interest and therefore, when the numerator has a sharp minimum, does not allow the associated maximum in η to depart far beyond $b = \frac{1}{2}a$. On the other hand, it means that thrust is somewhat increased for a value of b greater than $\frac{1}{2}a$, and this consideration may need to be balanced against considerations of efficiency.

These remarks are borne out by figure 4, which compares the dependence of thrust and efficiency on θ and σ , calculated by this two-dimensional theory for four positions of the yawing axis (half-chord, three-quarter chord, full-chord or trailing edge, and five-quarters-chord). Of these four positions, the middle two permit better maintenance of good efficiency at the higher values of the frequency parameter $\omega c/U = 2\sigma$ based on the 'chord' $c = 2a$ (fore-and-aft dimension of fin section).

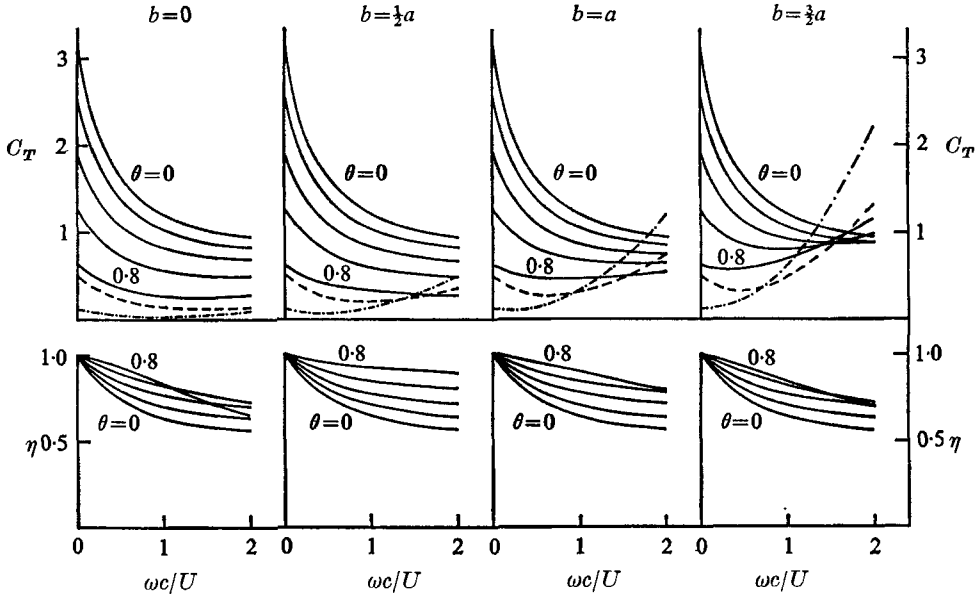


FIGURE 4. Thrust coefficient C_T and efficiency η predicted by two-dimensional aerofoil theory, for values 0, 0.2, 0.4, 0.6 and 0.8 of a feathering parameter $\theta = U\alpha/\omega h$, plotted as a function of $\omega c/U$ (which is 2σ), for different positions $x = b$ of the yaw axis (namely half-chord $b = 0$, three-quarter-chord $b = \frac{1}{2}a$, trailing-edge $b = a$, and a position 'five-quarters-chord', $b = \frac{3}{2}a$, beyond the trailing edge). -----, part of C_T for $\theta = 0.6$ predicted as coming from leading-edge suction. — · — · —, same for $\theta = 0.8$.

The thrust is represented by a thrust coefficient C_T equal to thrust per unit fin area divided by $\frac{1}{2}\rho(\omega h)^2$; thus, $C_T = \bar{P}/\omega^2 h^2 a$. (79)

This relates thrust to the amplitude ωh of the fin's lateral motion, and the reduction in C_T as $\omega c/U$ increases describes the decline in thrust from given fin movements at the lower forward velocities.

For the larger values of θ (say, 0.6 and 0.8) which are best for maintaining good efficiency, the thrust values are greater for the positions of the yawing axis which are farther downstream, and such positions might be tentatively preferred (for example, $b = a$ preferred to $b = \frac{1}{2}a$) as maintaining thrust better at the lower forward velocities. Some caution is needed here, however. For $\theta = 0.6$, the broken line shows which part of the thrust comes from leading-edge suction, the remainder being due to the backwardly inclined component of side-force. The chain-dotted line does the same† for $\theta = 0.8$. (Note that for $\theta = 0$, by

† In the case of the $b = 0$ diagrams, these are the only changes from figure 9 of Lighthill (1969).

contrast, there is no inclining of the fin and *all* the thrust predicted is due to leading-edge suction.)

Evidently, the increase of thrust as b increases, calculated for the larger values of θ and of $\omega c/U$, is entirely due to a steep increase in the leading-edge-suction component, whereas the element of backwardly inclined sideforce falls off, and may even become negative. When we question how it can become negative, we soon find that it is due to the second term in parenthesis in (74), which arises from the sideforce (70) acquiring an imaginary part from the $-i\omega^2\alpha b$ term in equation (61) for B . This can be thought of as a virtual-mass contribution to sideforce, due to rate of change of lateral momentum of water adjacent to the fin and swept from side to side by it, so fluid inertance plays a substantial role here as in elongated-body theory. The farther the yawing axis is behind the aerofoil centroid, the more this contribution to sideforce is negatively correlated with backward inclination of fin.

This tendency towards a reduced thrust contribution from backwardly inclined sideforce as b increases is more than made up, however, by the increased suction force, that is, the term in (74) proportional to $|A|^2$. It is the growth in the real part of A (see (69)) as b increases, associated with fluctuations in sideforce (70) out of phase with the fluctuations in angle of incidence, which increases this suction force.

These considerations indicate that attempts to achieve high thrust coefficients C_T from a two-dimensional aerofoil by choice of a yawing axis behind the trailing edge (such as the $b = \frac{3}{2}a$ choice in figure 4) are probably inadvisable quite apart from considerations of efficiency. They depend too much on realizing a very high suction force at the rounded leading edge, and if owing to separation only part of that force were realized the total thrust (including a negative component from backwardly inclined sideforce) would be very greatly reduced. Probably an optimum from thrust considerations as well as from efficiency considerations lies somewhere between $b = \frac{1}{2}a$ and $b = a$, which in practice means very close to the trailing edge.

This conclusion is, perhaps, relevant to why the lunate tail should be hydro-mechanically efficient. If a caudal fin were yawing as a whole about a single axis, with yaw angle in phase with its velocity of lateral translation, and if two-dimensional theory could be applied to each section, then good thrust with good efficiency would best be achieved if the axis of yaw were close to the trailing edge of each section. This requires that the trailing edge as a whole stretch almost straight along the axis of yaw.

Tapering of the fin must accordingly take place through the leading edge being bowed forward. Any bowing of the trailing edge should be small by comparison. We recover here the concept of a vertical trailing edge where angle of yaw and lateral velocity are perfectly in phase, which was a favoured idealization also in § 2.

This degree of departure from 'straight wing' conditions suggested as optimum by two-dimensional theory, with leading edge bowed forward but trailing edge practically straight, is in the right direction (see figure 6 of Lighthill 1969), although it does not go far enough; possibly a fully three-dimensional theory

might explain the fact that most lunate tails have also a trailing edge bowed forward (though not as much as the leading edge). In any case a properly worked-out two-dimensional theory is necessary as a preliminary to a more thorough three-dimensional study, using lifting-line techniques, of the advantages of a lunate-tail configuration.

Further discussion of three-dimensional aspects of the flow is not here attempted, but we conclude with some remarks about the appropriateness within two-dimensional theory of the linearization of boundary conditions, used in this section as well as in the earlier sections concerned with elongated-body theory. Extension of elongated-body theory to large-amplitude motions seems feasible, as mentioned in §1, but the problems of carrying out such an extension for even a two-dimensional theory of the lunate tail appear far from straightforward.

This is not to say that linearized theory is useless for evaluating the large-amplitude lunate-tail motions that are actually found (Fierstine & Walters 1968). Aerofoil characteristics at amplitudes relatively large, but below those where catastrophic stalling occurs (which fishes may be presumed to avoid), are often indicated reasonably well by extrapolation of small-amplitude characteristics. Nevertheless, one would like both to understand any tendency for thrust and efficiency to continue to follow curves predicted by linearized theory, and to estimate deviations from them.

A theory might be attempted for well-feathered oscillations of a two-dimensional aerofoil, making large displacements but combining them with such variations in angle of incidence that disturbances to the uniform stream of velocity U could still be regarded as small. Then a pressure

$$p - p_0 = -\rho(\partial\phi/\partial t + U \partial\phi/\partial x) \quad (80)$$

linearly related to velocity potential (as in (59) and (60) but now with ϕ not $\phi e^{i\omega t}$ as velocity potential), could still be used, and p would satisfy Laplace's equation and be continuous even across the vortex wake. The normal derivative of p at all points of the aerofoil surface would be known at each instant as the rate of change following a fluid particle of the normal velocity specified by the boundary conditions. For a flat-plate aerofoil, p could then be deduced in a form constituting a generalization of (63), and involving one arbitrary constant A that now would be a general function of time. This function would have to be determined by specifying that the solution of equation (80) for ϕ , got by integrating along lines on which y , z and $x - Ut$ are constant, satisfied the aerofoil boundary condition.

That last step, leading to the generalization of equation (66), would involve extremely complicated integrations, but the whole would be easier, perhaps, than a method which sought to calculate the velocity field induced by a sinusoidal vortex wake with amplitude approaching half a wavelength (Fierstine & Walters 1968). Methods of this latter kind cannot be ruled out, however, in any future efforts at achieving a three-dimensional non-linear theory, possibly using the idea (Lighthill 1969) that the lunate tail may generate a wake consisting of a succession of vortex rings. That ultimate development, however, would call for

something like the genius that Goldstein (1929) showed when he calculated the effect of the helicoidal vortex wake behind a propeller.

The author acknowledges with gratitude and pleasure the benefits of having sat for seven years at the feet of Sydney Goldstein.

REFERENCES

- FIERSTINE, H. L. & WALTERS, V. 1968 *Mem. S. Calif. Acad. Sci.* **6**, 1.
FLACHSBART, O. 1935 *Z. angew. Math. Mech.* **15**, 32.
GARRICK, I. E. 1957 In *Aerodynamic Components of Aircraft at High Speeds* (ed. A. F. Donovan & H. R. Lawrence), pp. 658-793. Princeton University Press.
GOLDSTEIN, S. 1929 *Proc. Roy. Soc. A* **123**, 440.
GRAY, J. & HANCOCK, G. J. 1955 *J. Exp. Biol.* **41**, 135.
KRAMER, E. 1960 *Z. Wiss. Zool.* **163**, 1.
LIGHTHILL, M. J. 1951 *Aeron. Quart.* **3**, 193.
LIGHTHILL, M. J. 1958 *Fourier Analysis and Generalized Functions*. Cambridge University Press.
LIGHTHILL, M. J. 1960 *J. Fluid Mech.* **9**, 305.
LIGHTHILL, M. J. 1969 *Ann. Rev. Fluid Mech.* **1**, 413.
POSSIO, C. 1938 *Aerotecnica*, **18**, 441.
ROBINSON, A. & LAURMANN, J. A. 1956 *Wing Theory*. Cambridge University Press.
TAYLOR, G. I. 1952 *Proc. Roy. Soc. A* **214**, 158.
WU, T. Y. 1961 *J. Fluid Mech.* **10**, 321.